Received: 11 July 2023 | Revised: 30 October 2023 | Accepted: 9 November 2023

DOI: 10.1002/fft2.335

FOOD FRONTIERS Open Access

REVIEW ARTICLE

Applications of Raman spectroscopy in clinical medicine

Yaping Qi[1,2] | Esther Xinyi Chen[3] | Dan Hu[1] | Ying Yang[1] | Zhenping Wu[4] | Ming Zheng[5] | Mohammad A. Sadi[6] | Yucheng Jiang[7] | Kang Zhang[3] | Zi Chen[8] | Yong P. Chen[1,2,6,9]

[1]Department of Engineering Science, Faculty of Innovation Engineering, Macau University of Science and Technology, Macau SAR, China

[2]Advanced Institute for Materials Research (WPI-AIMR), Tohoku University, Sendai, Japan

[3]Faculty of Medicine, Macau University of Science and Technology, Macau SAR, China

[4]State Key Laboratory of Information Photonics and Optical Communications & School of Science, Beijing University of Posts and Telecommunications, Beijing, China

[5]School of Materials Science and Physics, China University of Mining and Technology, Xuzhou, China

[6]Department of Physics and Astronomy and Elmore Family School of Electrical and Computer Engineering and Birck Nanotechnology Center and Purdue Quantum Science and Engineering Institute, Purdue University, West Lafayette, Indiana, USA

[7]Jiangsu Key Laboratory of Micro and Nano Heat Fluid Flow Technology and Energy Application, School of Physical Science and Technology, Suzhou University of Science and Technology, Suzhou, Jiangsu, China

[8]Division of Thoracic Surgery, Brigham and Women's Hospital, Harvard Medical School, Boston, Massachusetts, USA

[9]Institute of Physics and Astronomy and Villum Center for Hybrid Quantum Materials and Devices, Aarhus University, Aarhus C, Denmark

Correspondence
Yaping Qi, Email: ypqi@must.edu.mo

Yucheng Jiang, Email: jyc@usts.edu.cn

Zi Chen, Email: zchen33@bwh.harvard.edu

Yong P. Chen, Email: yongchen@purdue.edu

Funding information
Macau Science and Technology Development Fund, Grant/Award Number: 0031/2021/ITP

Abstract

Raman spectroscopy is a nondestructive and highly effective technique for analyzing biological tissues and diagnosing diseases by providing detailed spectral information about the specific molecular structures of substances. Its efficacy in these applications has been widely recognized, making it a powerful tool in the field. This article presents a comprehensive overview of the latest developments in Raman spectroscopy and its wide-ranging applications in the diagnosis of critical diseases, such as cancer, infections, neurodegenerative diseases, and predicting surgical outcomes. It highlights the significant contributions of Raman spectroscopy in these areas, shedding light on its potential as a valuable diagnostic tool. This article delves into the advancements of Raman spectroscopy in biomedical sciences, with a specific focus on state-of-the-art techniques such as surface-enhanced Raman spectroscopy, resonance Raman spectroscopy, and tip-enhanced Raman spectroscopy. These techniques have shown great potential in various applications within the field. The article explores their use in ex vivo and in vivo medical diagnosis, covering topics such as sample collection, data processing, and the successful establishment of correlations between Raman spectra and biochemical information in specific diseases. Furthermore, the article discusses the

limitations of the current research and offers insights into potential future directions for further exploration in the field of Raman spectroscopy in biomedical sciences.

KEYWORDS
biomarkers, COVID-19, disease, optical biopsy, pathological diagnosis, Raman spectroscopy, tissue

1 | INTRODUCTION

The accurate and early disease detection shows distinct advantages in facilitating early and effective treatment, tracking the progress of treatment, slowing disease progression, and reducing mortality (Moghimi-Dehkordi & Safaee, 2012; Paci et al., 2005). For example, in colorectal cancer (CRC), the 5-year survival rate can reach 90% (Meyerhardt & Mayer, 2005) with diagnosing patients at an early stage. However, only 39% of patients with CRC are diagnosed at this stage, mainly due to missed identification of lesions and the underuse of screening (Favoriti et al., 2016). The same trend has also been observed in epidemiological investigations of other diseases, such as infectious (Asai et al., 2012; Ruan, 2020) and neurodegenerative diseases (DeKosky & Marek, 2003). Therefore, innovative and reliable detection technologies with high specificity and sensitivity are constantly sought for disease diagnosis and severity grading (Krone et al., 2010; Li et al., 2013). Optical diagnostic techniques have several advantages over other approaches, including reasonable objectivity, high speed, and low cost (Kim et al., 2020). Among the label-free and noninvasive optical methods, Raman spectroscopy is a powerful tool that can detect the biochemical components of biological tissues. It has attracted considerable attention for clinical applications because of its excellent performance, simplicity of operation, and sensitivity in detecting and grading of lesion tissues (Blake et al., 2022; Kumar, 2017; Santos et al., 2017). Raman spectroscopy is based on Raman scattering, by which it can identify the composition of multicomponent substances based on information on the characteristic molecular vibrations in the substance to be measured (Butler et al., 2016; Mulvaney & Keating, 2000). Interestingly, all critical components of human tissues (proteins, nucleic acids, and lipids) have corresponding characteristic peaks in the Raman spectra, which contain much information. Moreover, in lesioned tissues, intracellular molecular composition and structures may vary from a normal situation and continue to change as the disease develops, which suggests that the morphology and composition of cancerous tissues can vary at the cellular and molecular levels between periods. Molecular fingerprint information and its evolution can be easily obtained with high accuracy and sensitivity using spectroscopic techniques, providing a feasible method for accurate and noninvasive detection (Feng et al., 2018). The capability of Raman spectroscopy makes it suitable for diagnosing progressive diseases, such as cancer, precancerous lesions (Favoriti et al., 2016; Meyerhardt & Mayer, 2005; Moghimi-Dehkordi & Safaee, 2012), infectious diseases (coronavirus disease [COVID-19], dysentery, dengue fever, and epidemic hepatitis) (Jadhav et al., 2021; Khan et al., 2016; Yuen & Liu, 2012), and metabolic diseases (osteoporosis, diabetes, etc.) (Guevara et al., 2018; Kochan et al., 2013; Morris & Mandair, 2011). These examples demonstrate the great potential of Raman spectroscopy in biomedical sciences. However, some limitations and challenges exist. For example, the spontaneous Raman scattering signal is weak and often subject to interference from other signals in practical applications. Moreover, the intense fluorescence background in biological samples can further minimize the signal-to-noise ratio (SNR) of Raman spectra. The weak nature of Raman scattering can be overcome by using localized surface plasmon resonance in surface-enhanced Raman spectroscopy (SERS) and tip-enhanced Raman spectroscopy (TERS), resonance Raman effect, stimulated Raman effect in stimulated Raman spectroscopy (SRS), and coherent anti-stokes Raman scattering (CARS). Another challenge is the slow speed of Raman spectroscopy because obtaining a spectrum with an acceptable SNR can take a long time, which is not conducive for spectral acquisition and fast imaging. Fortunately, this issue can be overcome by using nonlinear Raman techniques such as SRS and CARS, which offer video rate monitoring of biomolecules in live cells and tissues.

Previous reviews of Raman spectroscopy in medical applications have typically focused on only one part of disease management, including diagnosis (Favoriti et al., 2016), guiding surgeries (Santos et al., 2017), assessing treatment results (Paidi et al., 2019), or concentrated on only one or a group of certain diseases (cancers and bacterial infections, etc.) (Paraskevaidi et al., 2021), and are commonly limited to a single type of sample, such as biofluids (Lohumi et al., 2017), cells (Bonifacio et al., 2015), and tissues (Smith et al., 2016). Moreover, many previous studies on Raman applications aimed at improving instrument performance for better accuracy and sensitivity, whereas some of the improvement methods might not be applicable in detecting biological tissues as additional light sources that may damage samples (Choo-Smith et al., 2002; Smith et al., 2016). This review systematically evaluated the applications of Raman technology in various aspects of disease management, different types of diseases, and multiple samples. We summarize the recent advances in Raman spectroscopy for ex vivo and in vivo tissue diagnoses over the past decade and explore the balance between the accuracy and feasibility of the test from a medical perspective. Finally, the current challenges, difficulties, and future perspectives of Raman spectroscopy for clinical applications are presented.

2 | METHODS

2.1 | Use of Raman spectroscopy in ex vivo and in vivo detection

2.1.1 | Application of Raman spectroscopy in ex vivo tissue detection

In vivo research and its clinical applications are based on ex vivo studies. In detecting ex vivo tissues with Raman spectroscopy, a typical operation is the spectroscopic acquisition and analysis of ex vivo samples from humans and animals. In diagnostics, Raman spectroscopy is considered an alternative technique and complementary tool for tissue biopsy (Lizio et al., 2021). Numerous analyses using this tool have been performed on liver (Kochan et al., 2013), cervical (Rubina & Krishna, 2015), brain (Bury et al., 2019; Fu et al., 2008), lung (Song et al., 2020), breast (Brozek-Pluska et al., 2018; Li et al., 2017), and skin (Ali et al., 2013; Rangaraju et al., 2019) tissues. The studies primarily aimed to identify the differences in chemical components in various tissues, and the main factor that affected the results was sample preparation. Although the nondestructive and label-free detection characteristics of Raman spectroscopy allow fresh biological samples to be used without handling procedures (Santos et al., 2017), certain preprocessing techniques are still required for retrospective studies (Ali et al., 2013; Li et al., 2017). Various samples, such as fresh, formalin-fixed paraffin-embedded (FFPE), and frozen tissues, have been used for Raman spectroscopy–based pathological diagnoses (Brozek-Pluska et al., 2018; Li et al., 2017; Rangaraju et al., 2019). These three sample types have different advantages and limitations. In general, a fresh tissue is an ideal sample. However, its composition and structure may change once the tissue is excised. Maintaining the sample in a state similar to that in vivo in practical experiments is difficult. A significant challenge is maintaining the state of cells to simulate living tissues. Previous studies have presented several solutions to this challenge. Malini et al. (2006) soaked tissue sections in cold saline to shortly maintain the morphology of the cells and keep the sample moisturized. This study demonstrated that the Raman spectra did not display any changes from the fresh tissue spectra under these conditions. Additionally, Malini et al. considered the effect of osmolarity but did not account for the difference in pH between saline and body fluids. Fu et al. (2008) conducted a similar study using phosphate buffer at a pH similar to that of body fluids instead of saline, thereby avoiding the denaturation and aggregation of biological macromolecules caused by changes in acidity or alkalinity. Subsequently, with the development of freezing technology, liquid nitrogen was used to preserve samples (Song et al., 2020). In clinical studies, the availability of an extensive tissue bank serves as a crucial resource for facilitating accurate improvements in on-site retrospective-related research (Ali et al., 2013), so reliable preprocessing is aimed at the long-term preservation of samples. However, the current FFPE operation may affect the biochemical composition and lead to changes in Raman spectra. Various chemical and digital dewaxing approaches could eliminate peaks of paraffin from the Raman spectra of tissues (Brozek-Pluska et al., 2018; Ibrahim et al., 2017; Meksiarun et al., 2017; Ning et al., 2021). Because the tissue preparation and dewaxing processes also eliminate some diagnostic biomarkers, these operations may add difficulties to the classification of tissues for clinical identification, and thereby, the identification of FFPE samples typically has lower precision than that of frozen tissues. Recently, Ning et al. (2021) reported that during sample preparation, some information of biochemical tissue was lost. However, some commonly utilized multivariate analysis approaches, such as partial least squares discriminant analysis (PLS-DA), principal component analysis (PCA), and PCA–linear discriminant analysis (PCA–LDA), can still effectively distinguish among invasive ductal carcinoma, ductal carcinoma in situ, and health tissue. Therefore, although the frozen or fresh tissue preserved complete qualitative and quantitative information about its composition, the spectral results from dewaxed tissues were able to distinguish lesioned tissues from normal ones.

Furthermore, tissue smears are becoming popular in clinical diagnosis, as more biomarkers are identified in biofluids that are linked to specific diseases. Recently, biofluid smears have been used for Raman-based diagnostics, including the blood (Happillon et al., 2015; Hobro et al., 2013), saliva (Hole et al., 2022), respiratory secretion (Ge et al., 2016), cervical tissue (Traynor et al., 2021), and tear smears (Choi et al., 2014; Hu et al., 2016). Generally, smear tests offer new noninvasive or minimally invasive detection options as they allow detection with sparse biological tissue and require less tissue than slices. However, the development of smear substrates is a complicated and lengthy process, and researchers are constantly attempting to develop substrates with low spectral impact (Birech et al., 2020; Otange et al., 2017). Additionally, substrates that provide uniform Raman spectra, without the need to consider the excitation wavelength, are expensive and beyond the affordability of many laboratories. To reduce the effect of the substrate on the blood smear spectrum and to increase the Raman signals, Otange et al. (2017) smeared a conductive silver paste consisting of a mixture of solvent resins and silver metal particles on glass slides (with Ag being 35%–65% per weight), achieving excellent accuracy. The addition of "silver paste/paint" on the surface of a material for Raman spectroscopy is considered SERS, which is a common practice to enhance the Raman signals. Similarly, Birech et al. (2020) reported low-cost smear substrates coated with conductive silver paint that are useful in screening metabolic diseases of whole blood samples through Raman spectroscopy. By applying blood onto a glass slide coated with conductive silver paint, Raman signals were enhanced by a factor of 1.7 in comparison to the thick blood smears on regular glass slides. These results suggested that the background signals originating from these paste smear substrates had minimal impact on the Raman signals of blood samples and suppressed the photoluminescence signals from glass. They also used this smear for Raman spectroscopy to screen blood samples for type 2 diabetes (Birech et al., 2017). Moreover, other excellent materials that achieve low interference and repeatability are available, such as Raman-grade calcium fluoride (Githaiga et al., 2020), aluminum-coated substrates (Cui et al., 2016), stainless steel, potassium bromide, magnesium fluoride, and sodium chloride. However, elemental fluoride and fluoride ions are also highly toxic as they disrupt cell enzymatic processes, such as the transformation of

carbohydrates and lipids as well as synthesis of hormones, thus inhibiting tissue respiration.

It is worth noting that SERS is also promising in lateral flow assays for point-of-care applications and multiplexing platforms for both tissues and biofluids. For example, it has been demonstrated to be useful for the detection of bacteria and antibiotic susceptibility testing (Dina et al., 2023). Additionally, SERS has shown potential for early Alzheimer's disease (AD) diagnosis and the quantitative detection of multiple exosomes in clinical samples, enabling precise cancer diagnostics (Su et al., 2023; Zhang et al., 2023). Moreover, the capability of SERS in the multiplexed detection of multiple biomarkers keeps improving (Cutshaw et al., 2023).

2.1.2 | Application of Raman spectroscopy for in vivo tissue detection

Raman spectroscopy is not only highly accurate for detecting ex vivo biological tissues, but it also provides robust data and a technical foundation for in vivo biological studies. Biological in vivo testing uses a living individual to analyze the physical or chemical interactions between the testing instrument and the whole living organism or the local area (Kumar, 2017). This method can obtain realistic results without affecting the physiological state of an organism.

The application of Raman spectroscopy to biological in vivo testing has been developed based on ex vivo experiments. Raman spectroscopy can be applied directly to live tissue detection without processing or marker injection (Kumar, 2017). In this process, in vivo Raman data collection is achieved using a portable Raman system and Raman probes. These data can be used to construct diagnostic models and validate the application of Raman-based in vivo detection. The current application of Raman spectroscopy in clinical in vivo detection involves two main approaches. The first is a minimally invasive approach using a Raman system combined with medical endoscopy to achieve in situ detection (Almond et al., 2014; Huang, Teh, et al., 2010; Jeong et al., 2015; McGregor et al., 2017; Shu et al., 2021; Wang et al., 2015a, 2015b). This method detects and measures body tissues, including the respiratory system (McGregor et al., 2017; Shu et al., 2021) and digestive system (Almond et al., 2014; Huang, Teh, et al., 2010; Wang et al., 2015a, 2015b). The second is the direct detection of living tissue using the Raman system, as the endoscope may not reach the lesion sites (Guze et al., 2015; Jermyn et al., 2015; Krishna et al., 2014; Matthäus et al., 2018; Singh et al., 2013). Raman spectroscopy has been studied for cervical cancer and preterm birth in both human and animal models (Masson et al., 2022; O'Brien et al., 2014). Furthermore, spatially offset Raman spectroscopy has been shown to be useful for noninvasive skin cancer screening (Vardaki et al., 2023).

In general, there are several typical parameters used for Raman measurements in in vivo applications, including laser wavelength, laser power, integration time, and spectral range. When applying Raman spectroscopy in vivo to a specific tissue type or disease, several factors need to be considered. These factors include tissue thickness and composition, as well as disease-specific considerations. Tissue thickness can affect the penetration depth of the laser and the resulting Raman signal. Thicker tissues may require longer integration time or different techniques to obtain meaningful data. Additionally, different tissues possess varying levels of endogenous fluorophores, Raman-active molecules, and scattering properties. These variations can influence the spectral quality of the Raman signal and the SNR. Furthermore, certain conditions or diseases may introduce additional challenges or safety concerns for in vivo Raman measurements. It is crucial to address these considerations to ensure accurate and safe measurements. Therefore, when conducting in vivo Raman measurements, it is essential to carefully select the parameters to maintain a balance among safety, optimizing SNR, and accounting for tissue-specific variations.

2.2 | Raman spectra acquisition enhancement techniques

Raman spectroscopy–assisted endoscopy has gradually become a complete system, based on previous studies, especially image-guided Raman endoscopy. However, it is worth noting that the sensitivity of conventional/confocal Raman spectroscopy is usually low because of the weak nature of Raman scattering (typically 1 in 10 million photons are Raman scattered). But the sensitivity of Raman spectroscopy can be enhanced using special techniques. Therefore, different types of Raman signal enhancement techniques have been developed to improve the intensity of Raman signals (Rostron & Gerber, 2016). For example, SERS (Cialla-May et al., 2017; Le Ru et al., 2006; Nicolson et al., 2018; Zhang, Hao, et al., 2018), RRS (Liu et al., 2020), and TERS (Bonhommeau et al., 2022; Sonntag et al., 2014; Verma, 2017; Wang et al., 2017) are often used to enhance the sensitivity of detection and/or improve the spatial resolution. TERS, which can detect the vibration of a single molecule, has been widely employed for the optical analysis of biological tissue (Bonhommeau et al., 2022; Sonntag et al., 2014; Verma, 2017; Wang et al., 2017). These novel techniques demonstrate high biochemical sensitivity and selectivity, indicating that they are promising for biological and medical applications. Table 1 summarizes the principles, advantages, and limitations of five commonly used Raman techniques.

Previously, flexible endoscopes (Van Heel, 1954) relied on white light reflectance and were the standard instruments for cancer detection and precancer surveillance in internal organs (Brenner et al., 2001). However, detecting premalignant lesions and early neoplastic changes has presented a clinical challenge. Reliance on subjective visual diagnostic criteria, which primarily focus on structural and morphological tissue details, has resulted in poor diagnostic accuracy. This is because early neoplastic transformation often lacks noticeable morphological changes, making them difficult to detect even for experienced endoscopists (Areia et al., 2008). New techniques to improve detection accuracy and sensitivity by the observation of endogenous fluorophores in tissues and improving the contrast of the tissue microvasculature are beginning to be applied clinically. One outstanding result is narrow-band imaging (NBI) (Figuero, 2019; Robert, 2009;

TABLE 1 Principles, advantages, and limitations of the five basic Raman techniques used to enhance Raman signals under two classifications.

Classifications	Types	Theoretical foundations	Advantages	Disadvantages	References
Coherent Raman spectroscopy	CARS	Four-wave mixing	Almost no fluorescence interference; high imaging sensitivity and speed; strong signal intensity	Signal is affected by a co-generated coherent background signal, diffraction-limited resolution (typically 200–300 nm)	Aljakouch et al. (2019), Krafft et al. (2012), Zhang, Wang et al. (2022)
	SRS	Four-wave mixing	Superior in maintaining undistorted Raman spectra; high imaging sensitivity and speed; strong signal intensity; low detection limit	Signal is affected by co-generated coherent background signal, diffraction-limited resolution (typically 200–300 nm)	Figuero (2019), Robert (2009), Zhang et al. (2021)
Enhanced Raman spectroscopy	RRS	Resonance effect	Suitable for biological chromophores; high signal-to-noise ratio; selective signal enhancement	Chemical groups that do not participate in the electronic transition cannot be observed; fluorescence interference, diffraction-limited resolution (typically 200–300 nm)	Robert (2009), Albrecht (1961)
	TERS	Local optical, electromagnetic field enhancement	Allow detection in tiny feature sizes; high sensitivity with nanoscale spatial resolution typically in the range of 1–50 nm	The high spatial resolution in the *z* direction does not necessarily result in an equivalent resolution in the *x*–*y* direction	Kolhatkar et al. (2018), Kumar et al. (2017), Kumar et al. (2019), Mrđenović et al. (2022), Mrđenovicét al. (2023), Pandey et al. (2021)
	SERS	Chemical enhancement via charge transfer; electromagnetic enhancement	High probability of obtaining Raman enhancement; high sensitivity; low detection limit	Stringent requirements for analytes and substrates, diffraction-limited resolution (typically 200–300 nm)	Kolhatkar et al. (2018), Jones et al. (2019), Sitjar et al. (2021)

Abbreviations: CARS, coherent anti-stokes Raman scattering; RRS, resonance Raman spectroscopy; SERS, surface-enhanced Raman spectroscopy; SRS, stimulated Raman spectroscopy; TERS, tip-enhanced Raman spectroscopy.

Zhang et al., 2021). Huang, Bergholt et al. (2010) used this NBI-guided Raman spectroscopy to diagnose gastric dysplasia in vivo. A diagnostic sensitivity of 94.4% and a specificity of 96.3% were achieved using the Raman spectral differences between normal and dysplastic gastric tissues. Moreover, they identified albumin, phospholipids, nucleic acids, and histones as the most significant features in constructing the diagnostic model (Bergholt et al., 2014). Bergholt et al. (2011) have reported the implementation of NBI-guided Raman endoscopy for the first time. The results indicated that significant Raman spectral differences reflecting the distinct composition and morphology in the nasopharynx and larynx should be essential parameters in the interpretation. However, the specificity and sensitivity of these two studies differed significantly, which was most likely caused by the intensity difference of the Raman signals in different human tissues.

Autofluorescence imaging (AFI) is another promising, wide-field imaging modality. However, these wide-field imaging modalities still suffer from insufficient diagnostic specificity owing to a lack of ability to reveal specific biomolecular information regarding the tissue. The integration of Raman-based technologies with other optical modalities provides an excellent solution to overcome this limitation. For example, Lin et al. (2018) generated an integrated four-modality endoscopy system that combined white-light interferometry, AFI, diffuse reflectance spectroscopy, and Raman spectroscopy technologies. This system was utilized for in vivo endoscopic cancer detection, which achieved both high diagnostic sensitivity (98.6%) and high specificity (95.1%) for differentiating cancer from normal tissue sites. Jeong et al. (2015) introduced a novel dual-modal fluorescence-Raman endomicroscopic system that combines the use of fluorescence and SERS nanoprobes (Figure 1a,b). This innovative system was applied to simultaneously detect two important biomarkers, namely, human epidermal growth factor receptor (EGFR) 2 and EGFR, in a breast cancer orthotopic model (Figure 1c–f). Furthermore, Kim et al. (2017) extended the

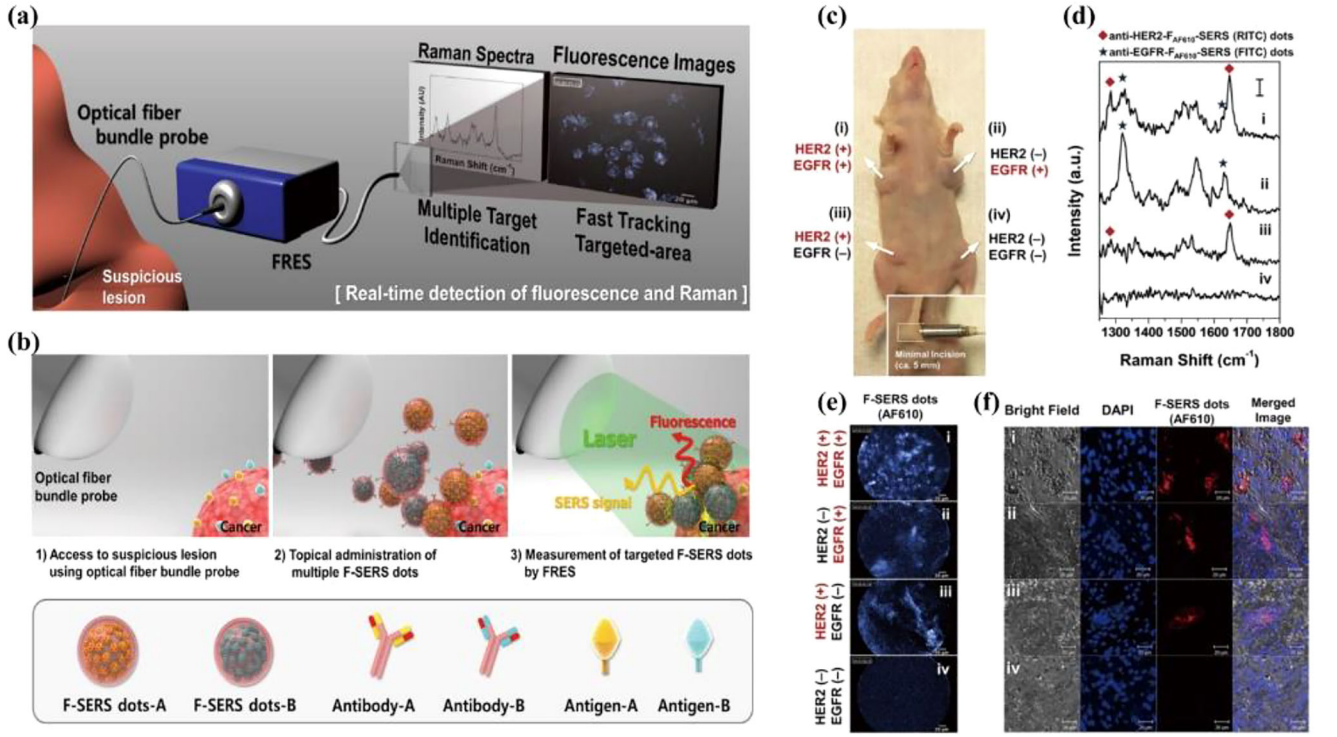

FIGURE 1 (a and b) Schematic illustration of applying the fluorescence-Raman endoscopic system (FRES) and surface-enhanced Raman scattering (SERS) nanoprobes for real-time multiplexed imaging: (a) Use of real-time fluorescence imaging to track the position of the probe-target region and SERS spectroscopic analysis to identify the target species. (b) Overview of the multiplexed molecular imaging process in vivo. (c–f) Description of an active in vivo targeting ability of the F-SERS dots on the epidermal growth factor receptor (EGFR) and human epidermal growth factor receptor 2 positive (HER2+) breast tumor xenografts: (c) Mice with tumors and the expression profile of their receptors. (d) Raman spectra generated through FRES. ★, fluorescein isothiocyanate (FITC), ◆, Raman band indicating rhodamine B isothiocyanate (RITC). (e) Real-time fluorescence images using FRES. The target probes are shown by the bright areas. (f) Tumor sites shown by confocal fluorescent laser scan images. *Source*: Figures are reproduced from Jeong et al. (2015) with permission from Nature Portfolio, copyright 2015.

diagnostic potential of a fluorescence-Raman endomicroscopic system for diagnosing CRC in an orthotopic xenograft model (Figure 2). Developing minimally invasive or noninvasive advanced optical technologies that exploit the intrinsic biomolecular signatures of cells and tissues would represent a significant milestone in endoscopic diagnostics.

Generally, a contact device requires fewer detection sites than an endoscope does. The high flexibility of the contact Raman system allows the accurate prediction of the contour of the lesion site. It presents excellent prospects for evaluating treatment results and optimizing surgical protocols. For example, Desroches et al. (2015) performed a comprehensive characterization of a handheld Raman spectroscopy system with the aim of maximizing the extent of resected cancerous tissue during glioma surgery. In preliminary measurements conducted on tissue samples collected from 10 patients, it was found that necrotic tissue could be differentiated from vital tissues, including both normal and cancerous brain tissues, with an impressive accuracy of 87%. In a study by Jermyn et al. (2015), a hand-held contact Raman spectroscopy probe technique was proposed for the live and local detection of cancer cells in the human brain. Using this technique, Jermyn et al. precisely identified cancer cells, achieving an impressive sensitivity of 93% and specificity of 91%. Based on these impressive results with excellent accuracy, a surgical plan can be developed based on the contour and area of the lesion before open surgery. Additionally, the results can be evaluated by examining the margins of the tissue in situ after lesion removal.

More prospective studies have been successfully established in vivo using animal models. In most situations, the simultaneous detection of multiple biomarkers at an early stage offers additional advantages, such as improved diagnostic accuracy and treatment response. Compared with the commonly used fluorescence methods, the combination of handheld Raman spectroscopy and surface-enhanced resonance Raman scattering nanoparticles (NPs) overcomes the limitations of spectral overlapping and strong background autofluorescence (Faulds et al., 2004; Lee et al., 2007). For instance, Huang et al. (2016) evaluated the ability of a handheld Raman scanner guided by SERS NPs to identify the extent of microscopic tumors in a genetically engineered RCAS/tv-a glioblastoma mouse model. Although this study demonstrates the possibility of combining gold-silicon dioxide SERS NPs with a handheld Raman scanner to guide surgical resection, the entire SERS image could still not be acquired. However, an in vivo multiplex detection of actively targeted biomarkers, which is challenging, was achieved. Using SERS NPs capable of three multiplexing, Dinish et al. (2014) demonstrated that they can actively target the in vitro and in vivo detection of three intrinsic cancer biomarkers, including EGFR, CD44, and TGFβ II, in a

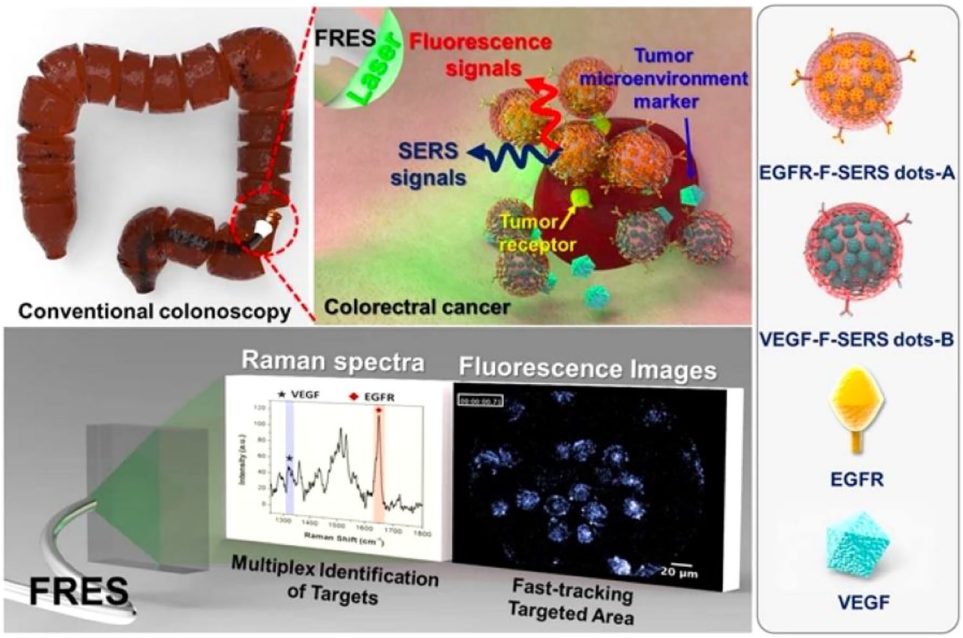

FIGURE 2 Diagram shows the application of Raman endoscopic system (FRES) for the in vivo multiplex molecular diagnosis of colorectal cancer. FRES was utilized to detect both the Raman signals and fluorescence for identifying tumors. *Source*: Figures are reproduced from Kim et al. (2017) with permission from Nature Portfolio, copyright 2017.

breast cancer model. Compared to Karabeber et al. (2014), Dinish et al. (2014) injected SERS NP into the tumor center rather than the veins to avoid the first-pass clearance effect of the liver to attenuate the SERS signal.

TERS has also been shown to be a promising technique in the biomedical field. For example, Kumar et al. (2017) reported the application of TERS for imaging small biomolecules, such as phospholipids, inside a biological cell with a spatial resolution of 20 nm. Pandey et al. (2021) reported the ability of TERS to visualize molecule disorder in lipid membranes with a spatial resolution of 20 nm. Interestingly, Mrđenović et al. (2022) demonstrated that TERS can be utilized to study the distribution of biomolecules on the cell membrane of breast cancer cells with a spatial resolution of less than 5 nm. More recently, Mrđenovicét al. (2023) showed the capability of TERS to detect biomolecules under ambient conditions at a sub-nanometer spatial resolution.

In summary, it is clear that Raman/SERS/TERS is a rapid, reproducible, and valuable tool in the minimally invasive early-stage diagnosis of critical diseases from blood serum and cellular samples with high accuracy. However, it is worth noting that oxidative stress processes might precede or indicate the preinstallation of pathological/neurodegenerative or oncological conditions. Their role in the interpretation of clinically relevant band assignments and specific biomarkers observed from the Raman/SERS spectra must be considered. This is because the spectral bands are also relevant in the diagnosis decision, as part of the malignant/critical conditions is presignalized by inflammatory processes. Therefore, a comprehensive analysis of the spectral data is necessary when applying Raman-/SERS-based methodology to clinical samples. For example, how is stage diagnosis affected by oxidative stress processes, and is the diagnosis decision made considering such processes?

2.3 | Data analysis and machine learning

Researchers have become increasingly interested in machine learning (ML)-assisted Raman spectroscopy analysis for biomedical applications, such as diagnosis, surgery, and disease treatment. Table 2 summarizes the recent advances in combining ML methods with Raman spectroscopy for these applications. ML combined with Raman spectroscopy for medical applications is an emerging research area in the health sciences. The accuracy of the information provided by Raman spectral data depends on the analysis and processing of the spectral data. Therefore, some basic preprocessing methods for spectral data, such as removing the fluorescence background, reducing noise, and correcting the baseline, remain important (Pence & Mahadevan-Jansen, 2016). Additionally, spectra normalization (e.g., spectral area, maximum value, and average intensity normalization) can reduce the effects of fluctuations in excitation intensity and better compare spectral shapes and relative peak intensities between different tissues. The analysis of the Raman spectra mainly includes two steps: spectral feature extraction and tissue identification. The diagnosis result may be affected if we analyze the entire spectral dataset because the initially collected data may contain considerable invalid and interfering information.

Each Raman peak represents the corresponding Raman shift and intensity. The substance components must be identified by attributing and comparing the spectral feature peaks that represent the

TABLE 2 Recent progress in integrating machine learning (ML) methods with Raman spectroscopy for biomedical applications: diagnosis, surgery, and disease treatment.

Applications	ML algorithms	References
Screening of cerebral ischemia and cerebral infarction	PCA, PLS, MRMR, SVM, KNN, PNN, DT	Fan et al. (2022)
Classify the types of isocitrate dehydrogenase mutations in gliomas	XGBoost, RBF-SVM	Sciortino et al. (2021)
Classification of glioma biopsies	RF, GB	Riva et al. (2021)
Alzheimer's disease (AD) identification based on saliva investigation	ANN	Ralbovsky et al. (2019)
Rapid screening of AD	SVM, RF, XGBoost, CatBoost	Wang et al. (2022)
Effective primary screening of COVID-19 by serum Raman spectroscopy	SVM	Yin et al. (2021)
Detection of COVID-19 infection by Raman spectroscopy of saliva	MILES	Ember et al. (2022)
Categorize breast cancer subtypes	PCA–DFA, PCA-SVM	Zhang, Li et al. (2022)
Breast cancer diagnosis	Ant colony optimization, QDA	Fallahzadeh et al. (2018)
Classify normal and cancerous breast tissue	CNN	Ma et al. (2021)
Diagnosis of lung cancer	CNN	Qi et al. (2021)
Lung cancer diagnosis based on the Raman spectra of exosome	ResNet-based deep learning model	Shin et al. (2020)
Screening of ovarian cancer	BPNN, PCA	Chen et al. (2022)
Predict gastric cancer	CNN, RF, SVM, KNN	Li et al. (2021)
Identification of kidney tumor tissue	SVM	He et al. (2021)

Abbreviations: ANN, artificial neural network; BPNN, backpropagation neural network; CatBoost, categorical boosting; CNN, convolutional neural network; DFA, discriminant function analysis; DT, decision tree; GB, gradient boosting; KNN, *K*-nearest neighbor; MILES, multiple instance learning via embedded instance selection; MRMR, minimum redundancy maximum relevance; PCA, principal component analysis; PLS, partial least squares; PNN, probabilistic neural network; QDA, quadratic discriminant analysis; RBF, radial basis function; RF, random forest; SVM, support vector machine; XGBoost, eXtreme gradient boosting.

corresponding Raman shifts and intensities. ML methods are suitable for capturing complex information from spectral statistics, and ML models can be utilized to identify the features of Raman spectra and classify substances (Lussier et al., 2020). Sciortino et al. (2021) examined mutations in isocitrate dehydrogenase (IDH) in gliomas. They extracted 2073 Raman spectra from 38 tumor tissues and screened 103 Raman shifts using an analysis of variance. The authors employed a support vector machine (SVM) with a radial basis function kernel (RBF-SVM) and eXtreme gradient boosting (GB) as classification models and used the intensity of each of these 103 Raman shifts as input features (Sciortino et al., 2021). Using cross-validation loops, it was determined that 52 of these shifts had the best discriminatory ability to distinguish between IDH-mutated and IDH wild-type mutations. The experimental results indicated that the RBF-SVM achieved a correct classification accuracy of 87% and XGB of 85%. Similarly, Riva et al. (2021) identified 135 Raman shifts as feature inputs and used GB and random forest models to classify glioma biopsies.

However, preprocessing and feature extraction are time-consuming and tedious when dealing with large-scale data. Deep learning is an excellent option to solve this problem (Lussier et al., 2020). Deep learning, as a subfield of ML, involves the use of end-to-end neural network that combines feature extraction and classification. Because all the layers of neural networks are trained together, deep learning models can automatically extract features and yield results (Lussier et al., 2020). In recent studies, convolutional neural networks (CNNs) have become popular deep learning models for Raman spectral analysis. Liu et al. (2017) evaluated several classical CNN architectures applied to Raman spectral data, including LeNets (ResNet). Ma et al. (2021) classified healthy and cancerous breast tissue using Raman spectroscopy combined with a CNN and achieved an overall accuracy of 92%. This experiment demonstrated that the CNN algorithm is more accurate than conventional ML algorithms when using a large dataset. Qi et al. (2021) transformed one-dimensional (1D) Raman data from lung tissues into 2D Raman spectra using a short-time Fourier transform and then used a CNN to classify and diagnose lung cancer. This study compared the classification accuracy of the CNN model with other ML models, such as PCA–LDA and SVM, where CNN, PCA–LDA, and SVM achieved an accuracy of 96.5%, 90.4%, and 93.9% in the test group, respectively (Qi et al., 2021). This study also proved that the deep learning model can significantly improve the performance of large data samples. The application of deep learning algorithms provides innovative ideas for Raman exploration of classification tasks, making this interdisciplinary area a current research topic.

3 | APPLICATIONS OF RAMAN SPECTROSCOPY IN MEDICAL SCIENCES

3.1 | Cancer and precancerous lesions

Cancer remains a leading cause of death and a critical barrier to increasing life expectancy worldwide (Hulvat, 2020). The effectiveness of cancer treatments depends on early detection and exact diagnosis. Numerous studies utilizing Raman spectroscopy have revealed the

entire process of cancer diagnosis and treatment, including the differentiation of precancerous tissue, cancerous tissue, and normal tissue in ex vivo samples (Depciuch et al., 2020), tumor staging (Bovenkamp et al., 2018), and predictions of surgical margins (Barroso et al., 2016). Here, we review its use in breast cancer, lung cancer, and CRC.

3.1.1 | Breast cancer

With 2.26 million new breast cancer cases in 2020, breast cancer has officially replaced lung cancer as the most prevalent cancer worldwide (Hulvat, 2020). Numerous studies have focused on exploring the usage of Raman spectroscopy to detect chemical changes in cancerous tissues (Depciuch et al., 2020). In a few early studies, researchers have examined the Raman spectra of breast tissues and applied fitting techniques to identify specific components within the tissue. These components include fat, collagen, cell nucleus, epithelial cell cytoplasm, calcium oxalate, calcium hydroxyapatite, cholesterol-like lipid deposits, and β-carotene. Based on this theory, a later study by Abramczyk and Brozek-Pluska (2013) revealed that the main differences between normal and cancer tissues were in the spectral regions associated with the vibrations of carotenoids, fatty acids, and proteins. Lyng et al. (2019) discriminated between breast cancer and benign tumors using Raman spectroscopy, and PCA was conducted to determine whether the spectra could be differentiated to their overall class of benign and cancerous tumors. The study indicated that several vibration modes significantly differed between benign and cancerous types, indicating the potential quantification of Raman spectroscopy for carcinoma grading.

Applying ML algorithms reduces the time required to extract and analyze the collected Raman spectra. The application of ML techniques to the classification of Raman spectra in breast cancer diagnosis has demonstrated promising results. In a study by Fallahzadeh et al. (2018), Raman spectra were combined with an ant colony optimization algorithm for breast cancer diagnosis. By selecting five features, the study achieved a categorization accuracy of 87.7% for normal, benign, and cancerous groups. Furthermore, Ma et al. (2021) employed a combination of Raman spectroscopy and CNN to simplify the analysis process. They developed a 1D-CNN model to classify the spectral data from healthy and cancerous breast tissues. The study compared the specificity and sensitivity of various spectral classifiers, including 1D-CNN, SVM, and FDA. The results reveal the potential advantages of the 1D-CNN model in achieving superior classification performance compared to other algorithms. Moreover, ML-assisted Raman spectroscopy has also been used for breast cancer prevention. Yala et al. (2019) developed a deep learning model based on full-field mammograms and traditional risk factors, which was more accurate than the Tyrer–Cuzick model (version 8), which is the current clinical standard. The precise risk assessment provided by this pioneering research may benefit patients when traditional risk factors such as family history are unavailable.

As Raman technology allows for minimally invasive and noninvasive testing, it facilitates the examination of body fluids or metabolites as a novel and effective method to diagnose breast cancer. For example, Pichardo-Molina et al. (2007) investigated serum samples obtained from patients diagnosed with breast cancer. Their findings confirmed the value of Raman spectroscopy as a valuable technique for minimally invasive diagnostics. Although these studies obtained specific bands that indicated group differences and could be used as potential screening markers for breast cancer, the underlying molecular mechanism of these differences among tissues at different stages remains unknown. Similarly, a series of later studies achieved metabolite profiling of human blood using Raman spectroscopy for surgery assessment or tumor screening in breast cancer. Lin et al. (2020) profiled blood samples from breast cancer patients at different treatment stages (pre- and post-surgeries) based on the relative concentrations of metabolites of patients post- and preoperatively. Label-free SERS technology has been used to evaluate the effects of surgery on breast cancer. Nargis et al. (2019) analyzed Raman spectroscopy from the same set of serum samples from breast cancer patients using SERS to distinguish different stages of breast cancer.

3.1.2 | Lung cancer

Lung cancer is the leading cause of cancer-related deaths (18.0%) (Hulvat, 2020). Despite advances in surgical, radiotherapeutic, and chemotherapeutic treatments, the long-term survival rate remains low (5% at 10 years for non-small cell lung cancer) (Barta et al., 2019). To date, the most recognized reduction in lung cancer mortality rates is related to early-stage diagnosis, followed by surgical resection. However, a high rate of false-positive results in screening using computed tomography is a significant challenge in the current detection method. Therefore, to maximize the benefits of screening for lung cancer, it is crucial to improve risk stratification using prediction models or biomarkers that can accurately assess the risk of developing the disease. Additionally, gaining a deeper understanding of the biological characteristics of aggressive cancers is essential. The emergence of Raman technology as a popular and efficient diagnostic tool has been supported by recent studies, which have demonstrated the valuable diagnostic information that Raman data from various samples can provide (Kong et al., 2015). Specifically, this article focuses on Raman data obtained from saliva, urine, blood, and exosome samples, presenting four distinct types of models for analysis and diagnosis. Human saliva contains abundant proteins and metabolites that allow for the diagnosis of certain diseases. Interestingly, Li et al. (2012) measured and differentiated saliva SERS readings from 21 patients with lung cancer and 20 healthy volunteers. The results indicated that most of the Raman peak intensities decreased in patients with lung cancer compared to those in the general population. These peaks were assigned to proteins and nucleic acids, which indicated a corresponding decrease in these substances in the saliva. A recent study by Qian et al. (2018) analyzed saliva samples from 61 patients with lung cancer and 66 healthy controls using an SERS system and a nano-modified chip. It summarizes 12 characteristic peaks of the spectral line in patients with lung cancer with an explanation of biochemical changes. Ke et al. (2022)

pooled and analyzed data obtained from relevant diagnostic studies in 2020. The pooled sensitivity and specificity in the saliva samples were 0.91 (95% CI 0.80–0.96) and 0.95 (95% CI 0.73–0.99), respectively, which indicated that Raman spectroscopy data in saliva samples provide accurate, sensitive guidance for early-stage lung cancer diagnosis. However, the susceptibility of saliva samples to sputum interference poses a challenge as it may bias the results.

Urine contains approximately 3000 proteins and is an ideal sample for protein and peptide biomarker studies. Several researchers have reported that urine proteome profiling can predict lung cancer in control cases and other tumors (Zhang, Leng, et al., 2018). Further studies on metabolomic analyses have confirmed that metabolites in urine can be used to diagnose lung cancer and assess prognosis (Mathé et al., 2014). Carrola et al. (2011) analyzed and verified several main metabolites contributing to lung cancer discrimination, including hippurate and trigonelline (reduced in patients), β-hydroxyisovalerate, α-hydroxyisobutyrate, *N*-acetylglutamine, and creatinine (elevated in patients relative to controls). Yang et al. (2014) achieved the facile and label-free detection of lung cancer biomarkers (adenosine) in urine using magnetically assisted SERS. Furthermore, the proposed SERS sequence allows high-throughput detection with high sensitivity. Despite this research suffering from the limitations of the metabolite category, the results demonstrate the valuable potential of metabolomics for identifying putative biomarkers of lung cancer in urine.

Previous studies have investigated plasma and serum levels of deoxyribonucleic acid (DNA) and ribonucleic acid (RNA) to detect the presence of cancer (Bratchenko et al., 2019). Because the Raman spectra of biochemical compounds produce high-dimensional multivariate datasets, many studies have confirmed the ability of different blood component samples to detect lung cancer. Guo et al. (2020) developed a highly selective detection system combining asymmetric polymerase chain reaction (PCR) and SERS for the evaluation of EGFR mutation genes in circulating tumor DNA in blood samples. In addition to venous whole blood samples, serum is the most used sample, as it is a cleaner sample typically free of cells and platelets (Bukva et al., 2021; Liu et al., 2019; Tahir et al., 2021; Wang et al., 2018). In another study (Wang et al., 2018), the Raman spectra of the sera of peripheral venous blood were measured using a micro-Raman spectrometer. The study included individuals from five groups, which encompassed healthy volunteers and patients diagnosed with non-small cell lung cancer in different stages. The study indicated a sequential reduction in Raman spectral intensity in serum samples from the control, stage I, stage II, and stage III/IV groups.

Compared to the abovementioned body fluids, exosomes present in these biofluids are considered more efficient biomarkers (Yamamoto et al., 2017). Owing to their natural location, membrane proteins of exosomes can be detected without exosome lysis (Han et al., 2019). Increasing evidence suggests that SERS can be used for exosome detection. Such detection can be divided into label-free exosome detection (Avella-Oliver et al., 2017; Park et al., 2017; Sivashanmugan et al., 2017) and exosome detection with SERS tags (Shin et al., 2018; Wu et al., 2021).

In general, label-free assays minimize the impact of target molecules on cells or tissues and allow information to be revealed in the native state of the sample. Additionally, although disease-associated extracellular vesicle (EV)-specific markers are unavailable, label-free SERS can identify unique patterns of disease-associated EVs through their molecular fingerprints (Rojalin et al., 2019). Park et al. (2017) have reported a label-free classification method for exosomes to detect lung cancer with 95.3% sensitivity and 97.3% specificity by combining SERS and statistical pattern analysis (Figure 3). They explained this difference by listing 11 points in SERS signals from lung cancer cell-derived exosomes. Even though the classification is not precise for an accurate blood sample containing many exosomes of different origins, and only a few exosomes are derived from cancer cells, trends have been established. Therefore, this serves as motivation for the subsequent research discussed below.

SERS tags, typically known as SERS-active nanoprobes, produce strong characteristic Raman signals and can be used to indirectly sense target molecules using laser Raman spectrometry or SERS microscopy, which demonstrate extraordinary features for bioanalysis. Several exosome analyses utilizing SERS have been recently reported. Shin et al. (2018) analyzed specific surface protein compositions of exosomes to diagnose cancer. This study suggested that the Raman bands of exosomes from non-small cell lung cancer cells correlated well with several protein markers, including CD9, CD81, epithelial cell adhesion molecule, and EGFR.

3.1.3 | CRC

CRC induced an estimated 1.9 million incidence cases and 0.9 million deaths worldwide in 2020 as the third most common malignancy and the second most deadly cancer (Sung et al., 2021). Current diagnostic tests rely on the histopathological analysis of tissue biopsies and suffer from limitations in their moderate diagnostic performance, invasiveness, and costly and laborious methodologies. Although Raman spectroscopy is not yet used in the routine clinical diagnosis of CRC, evidence of its strengths and prospects is increasing.

As mentioned in the previous section, Raman-based endoscopes are often used in prospective studies to detect digestive tract tissues (Almond et al., 2014; Huang, Teh, et al., 2010; Wang et al., 2015a, 2015b). Generally, an in vivo probe comprises a light source and an optical fiber probe. In this case, the probe can act as both a light source and a detector relaying a signal. The probes used in early studies were not practical for clinical diagnosis because of their long spectral acquisition time. Moreover, some of the materials that the probes are manufactured from have large Raman cross-sections, resulting in design SNR issues. However, with the development of probes over several decades, some recent studies have made progress in designing probes for gastrointestinal tissues using Raman-based endoscopy tests (Jayhooni et al., 2019; Short et al., 2016). In particular, Jayhooni et al. (2019) developed an endoscopic Raman spectroscopy device with side-viewing functionality that enables circumferential scanning spectral measurements inside thin conduits (Figure 4). The proposed device

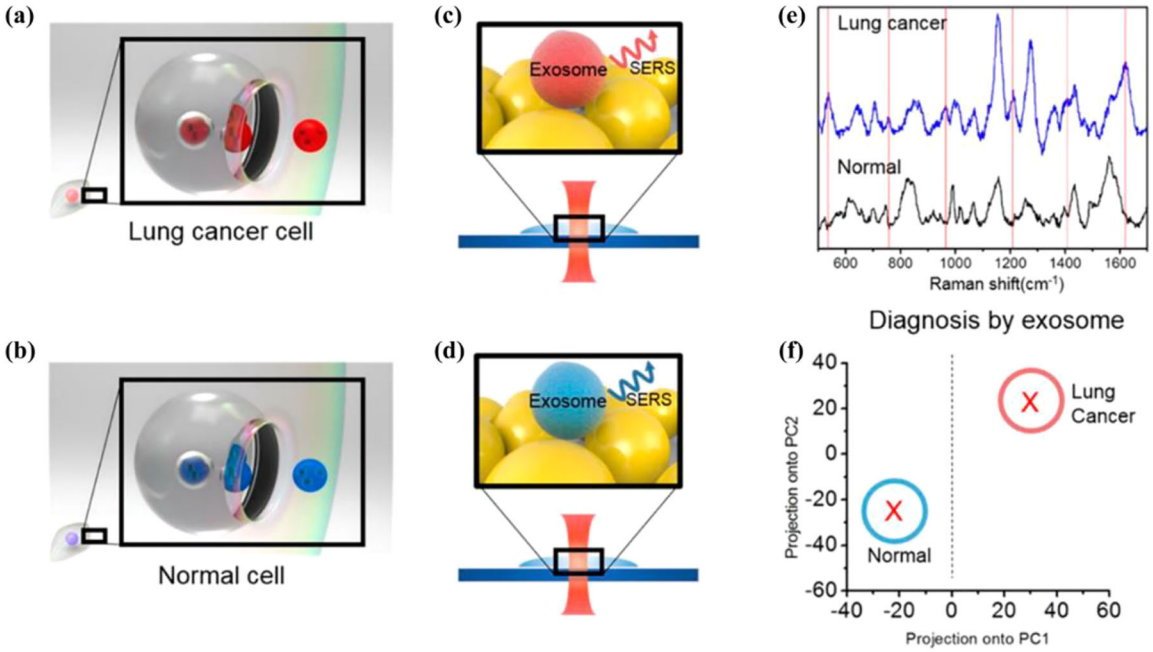

FIGURE 3 The application of surface-enhanced Raman scattering (SERS) categorization of the exosomes for the diagnosis of lung cancer. (a and b) Examples showing the release of exosomes from normal and lung cancer cells into the extracellular environment by fusing multivesicular endosomes to the plasma membrane. (c and d) Raman spectra were obtained using SERS on normal and lung cancer cell-derived exosomes. (e) The SERS spectra obtained using the approaches in (c) and (d). Red line shows the peak of the lung cancer-derived exosome. (f) Principal component analysis of the SERS spectra for the classification of exosomes. Samples in blue circles represent normal cell-derived exosomes, whereas red circles show lung cancer cell-derived ones. *Source*: Figures are reproduced from Park et al. (2017) with permission from ACS Publications, copyright 2017.

performed well in the detection of chemicals, harvested animal lung tissue ex vivo, a murine colon model in situ, and human skin in vivo. All the results demonstrated excellent agreement with the reported reference data while revealing >99% wavenumber accuracies. The advent of the side-view probe has the potential to address the limitations of conventional Raman endoscopy systems in terms of angle and detection range, as well as contributing to the screening of lesions in narrow lumens.

Another popular area of research that applies Raman technology to the CRC diagnostic process is liquid biopsy. Raman spectroscopy has exceptional potential for use in the analysis of biofluids for several reasons. One is water, which is the major component of all biofluids and is a very weak Raman scatterer. Therefore, many recent studies have focused on achieving CRC detection using the Raman signals of biomarkers in biofluids. Hong et al. (2020) employed gold NP (AuNP) colloids mixed with serum from patients with CRC to provide strong and stable SERS profiles. Their spectral analysis supported that patients with CRC have lower serum concentrations of tyrosine and hypoxanthine than healthy volunteers, which is in accordance with earlier metabolomic studies (Li et al., 2019; Long et al., 2017). However, the appearance of characteristic peaks is not directly associated with cancerous lesions, and precancerous lesions intermediate between healthy tissue and CRC were not considered in this study. Thus, once samples of precancerous lesions or other hyperplastic tissues are introduced, the accuracy of the proposed classification method will be negatively affected. In another study, Feng et al. (2015) utilized SERS to analyze blood plasma to detect CRC, considering adenomatous polyps. After generating the classification model with the PLS-DA method, the proposed model achieved a diagnostic sensitivity of 86.4% and a specificity of 80.0% for CRC and polyps, respectively, suggesting that biomolecular differences exist among the blood plasma samples of the CRC group, adenomatous polyp group, and regular volunteers. Moreover, the Raman spectroscopy of blood samples provides more information than the diagnostic basis for CRC. Both point mutations and deletions play a significant role in tumorigenesis, promotion, invasion, and metastasis of cancer, as well as in chemotherapy resistance (Minamoto & Ronai, 2001). The PCR-assisted Raman system makes performing genetic testing on tissue samples possible in order to explore individual drug resistance and guide the choice of treatment options. Li et al. (2018) developed a procedure based on PCR and SERS by amplifying DNA-containing target mutations and annealing probes to detect six mutations located in *BRAF*, *KRAS*, and *PIK3CA* in plasma samples from 49 patients with CRC. Although only two specific mutations were related to right-sided colon cancer in this preliminary study with a small sample size, and no extended discussion on associations between genetic mutations and individuals exist, the combination of PCR and Raman is still a prospective revelation because it allows early diagnosis before tissue lesions and demonstrates the potential to perform chemotherapy drug selection.

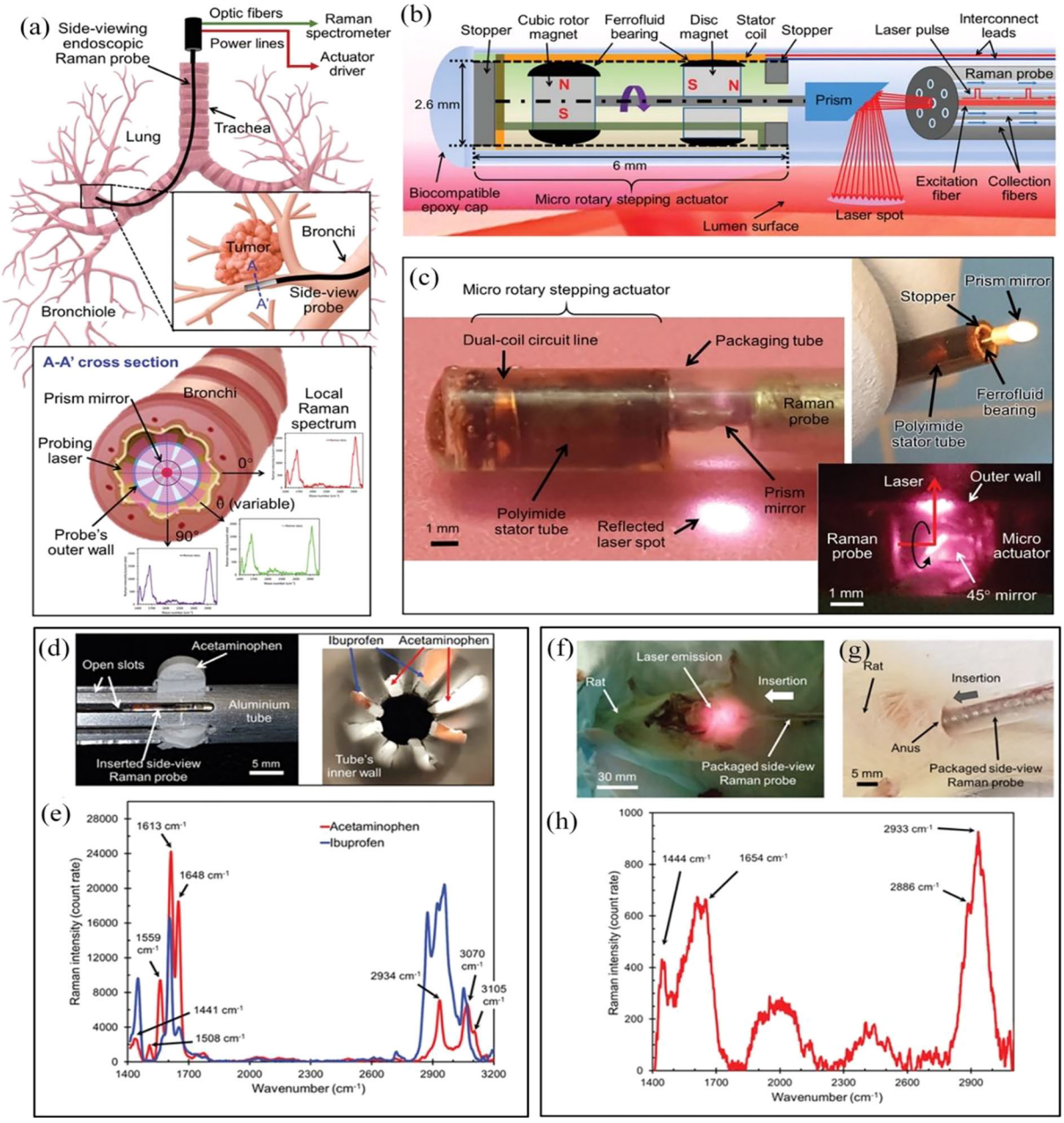

FIGURE 4 Schematic overview of the side-viewing endoscopic Raman spectroscopy device, angle-resolved chemical detection test, and in situ test. (a) A conceptual schematic of the side-view Raman device—specifically designed for the detection of peripheral lung cancer. (b) Schematic diagram of the construction of the side-view mechanism. (c) An overview of an integrated side-viewing Raman spectroscopy device. (d and e) Angle-resolved chemical detection test: (d) acetaminophen and ibuprofen samples were alternately loaded into the open slots of the tubular test device, and the figure on the right shows an axial internal view of the device with the two test chemicals. (e) The Raman signals of acetaminophen and ibuprofen samples were obtained stepwise, showing high accuracy of the measured peak positions. (f–h) In situ test using a rat colon model: (f) the side-view Raman probe was inserted into the colon of the euthanized rat, indicating emissions of the probing laser. (g) The side-viewing probe was inserted into the colon through the anus and rectum. (h) Raman spectrum obtained from the raw data. *Source*: Reproduced from Jayhooni et al. (2019) with permission from Wiley Online Library, copyright 2019.

3.2 | Infectious diseases

Infections caused by bacterial pathogens, viruses, and parasites are prevalent in clinical settings and are considered the top 10 most frequent causes of mortality globally (Bearman & Wenzel, 2005). In low-income countries and regions, sepsis, a disorder characterized by systemic inflammation secondary to infection, is a substantial contributor to mortality (Shrestha et al., 2017). Herein, we summarize the latest advances in Raman technology for diagnosing and evaluating infectious diseases.

3.2.1 | Pathogenic bacteria

Overall, Raman spectroscopy provides a whole-organism fingerprint, which is typically referred to as information regarding the chemical components and biomolecular configurations during bacterial sample analysis (Ashton et al., 2011). Currently, owing to the low concentration of bacteria in clinical samples, the majority of studies performing Raman spectroscopy on clinical bacterial pathogens require enrichment of disease-causing bacteria, and the most common practice is culture on agar plates (Kaewseekhao et al., 2020). However, as in other conventional detection methods for bacterial pathogens, which rely on medium culture (Váradi et al., 2017; Verroken et al., 2015), this inevitably takes a long time. The limited success in culturing certain bacteria can have a significant impact on the accuracy of experiment results due to the specific growth requirements of these bacteria. To overcome the limitations of time wasting, attempts to apply Raman spectroscopy to tissues for in situ diagnosis of infectious diseases have increased (Dhankhar et al., 2021). The application of SERS is a common method to improve the SNR, which enhances the intensity of the Raman signal and can be used as an alternative to concentrated culture of bacteria. Kelly et al. (2018) have reported a SERS-based system for the detection of chemisorbed methyl sulfide in the headspace of six live bacterial cultures (*Escherichia coli* DH5α, *E. coli* K12 WT, *Staphylococcus aureus* Cowan I, *Enterococcus faecalis* ATCC 10541, *Pseudomonas aeruginosa* OA1, and *Bacteroides fragilis* NCTC 9343) (Figure 5a) before and after the use of antibiotics (Figure 5b–i). As chemisorbed methyl sulfide can only be produced by living bacteria metabolizing dimethyl disulfide, the efficacy of antibiotics can be evaluated using multiple analyses. Although this study did not simulate the biochemical environment, it is still a promising step toward the bedside detection of bacterial infections and rapid antibiotic drug testing. Moreover, the detection of bacterial pathogens without culturing has been developed (Tien et al., 2018) to identify antibiotic-susceptible bacteria from antibiotic-resistant bacteria and diagnose mixed flora infections. Unfortunately, although SERS is considered an excellent analytical methodology, it has not yet been widely adopted as a routine diagnostic approach due to some limitations. The problem receiving the most attention is the production of appropriate substrates with distinct characteristics (Ouyang et al., 2017). In addition to bacterial infections, Raman spectroscopy has been applied to identify other microbial species, which has inspired the exact determination of parasites and viruses (Thomas, 1976).

3.2.2 | Pathogenic virus

The spread of pathological viruses remains a persistent public health issue. Considering the historical events in the public health field in the recent decades, arriving at such a conclusion is expected: Virus-related disease deemed containable can quickly escalate into a global calamity, such as the outbreaks of severe acute respiratory syndrome coronavirus 1 (SARS-CoV-1) in 2003 and the COVID-19 pandemics in 2019.

COVID-19 caused by SARS-CoV-2 has been declared a public health emergency of international concern by the World Health Organization (Cucinotta & Vanelli, 2020). The conventional samples commonly used for diagnostic testing of SARS-CoV-2 are nasopharyngeal and oropharyngeal swabs. However, as the sample collection process is prone to discomfort, recent studies have suggested that saliva could be an effective alternative (Xu et al., 2020). Azzi et al. (2020) analyzed saliva samples from COVID-19 patients using reverse transcription-PCR (RT-PCR). All the participants tested positive, demonstrating that saliva could be a valuable sample for COVID-19 diagnosis. Although RT-PCR has been successfully used to detect COVID-19, this method has a low sensitivity for SARS-CoV-2 detection before the onset of symptoms (Kucirka et al., 2020). Therefore, developing novel detection methods is crucial.

Carlomagno et al. (2021b) proposed a Raman spectroscopy–based saliva analysis method to differentiate SARS-CoV-2 infections. The deep learning–based Raman classification model applied in this study could distinguish patients with >95% accuracy. Ember et al. (2022) used innovative multi-instance learning-based ML and droplet segmentation methods to analyze the spectral data of salivary droplets. Experiments demonstrated that Raman spectroscopy could detect biomolecular changes in COVID-positive and COVID-negative saliva supernatants. Huang et al. (2021) exploited a residual neural network–based model to assist SERS analysis, which was used to detect SARS-CoV-2 antigen in pharyngeal swabs or sputum of COVID-19 patients. Figure 6a presents the detection process of this study, and the detailed model structure is demonstrated in part (b). The diagnostic accuracy of this method was 87.7%, which proves to be a promising approach to facilitate the rapid on-site diagnosis of SARS-CoV-2.

Additionally, serum has been investigated as a test sample (Han et al., 2020; Rabbani & Ahn, 2021). Goulart et al. (2022) investigated the Raman spectra of human serum samples, comparing those from individuals with COVID-19 to those from individuals without the disease. The discriminant analysis method used in this experiment classified the spectra with 87% sensitivity and 100% specificity. In a recent study, Paria et al. (2022) presented a new platform that combined SERS and ML to detect SARS-CoV-2 in large areas without labels. They performed the rapid detection of SARS-CoV-2 in a label-free manner by recording the SERS features of viruses on rigid and flexible substrates using plasma-active nanopatterning. This method provided test results within 25 min. Furthermore, the ongoing mutations of SARS-CoV-2 virus aim to evade the human immune system's defenses, exacerbating the challenge of controlling the COVID-19 pandemic (Garcia-Beltran et al., 2021). Pezzotti et al. (2022) identified significant vibrational differences between the Raman spectra of two British variant subtypes (QK002 and QHN001) present in Japan and the Japanese isolate (JPN/TY/WK-521), as illustrated in Figure 7a–c. The authors also used customized barcodes (Figure 7d–g) for Raman spectroscopy to represent viral variants to aid in electronic record-keeping and translate molecular features into instantly accessible information for users. This work illustrates that Raman spectroscopy could provide a clear understanding

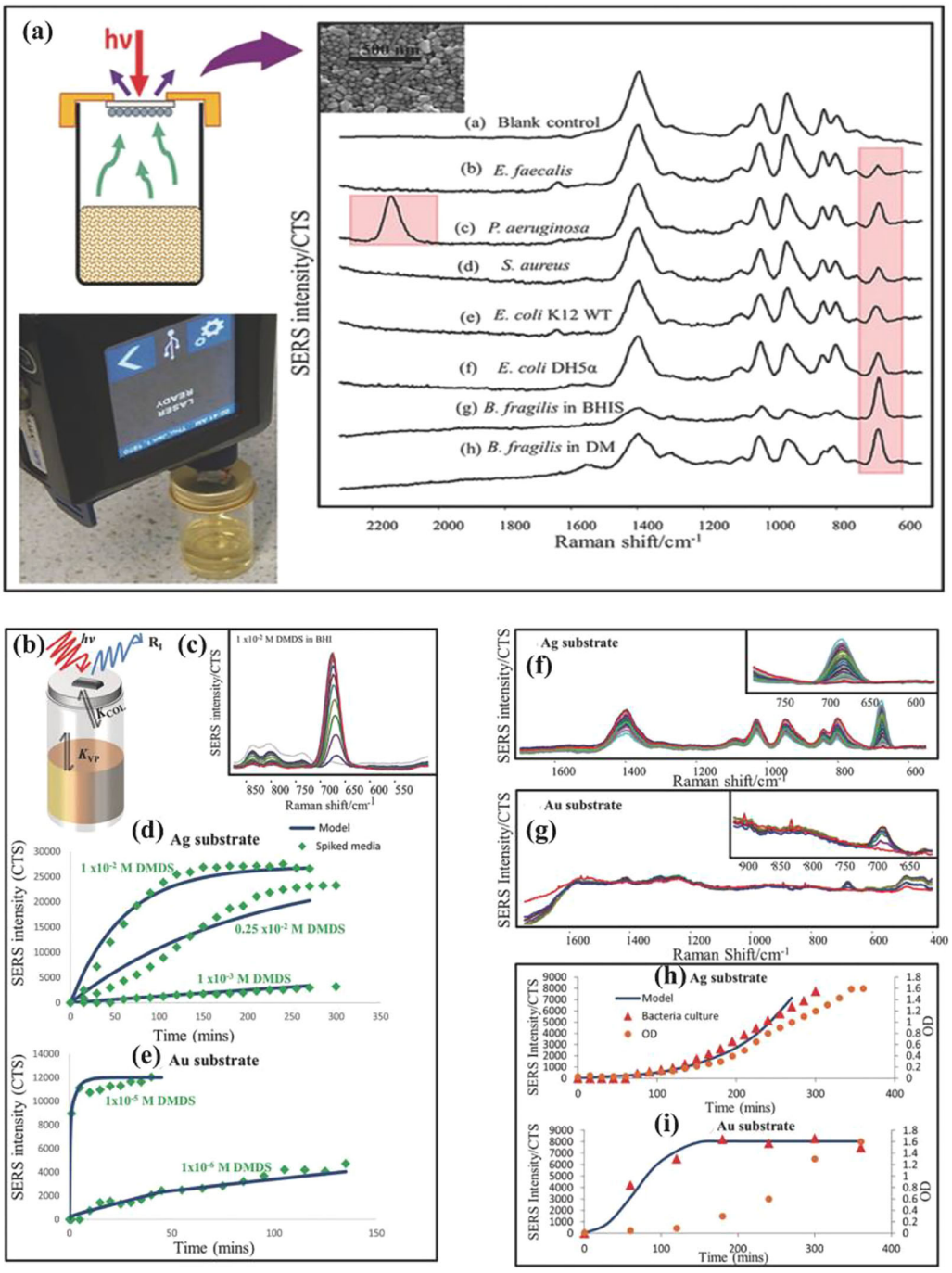

FIGURE 5 (a) Overview of the detection principle and configuration of headspace surface-enhanced Raman scattering (SERS) analysis and the SERS spectra of samples. (b) Illustration of the relationship between the dissociation equilibrium of dimethyl disulfide (DMDS) into the headspace and the adsorption of methyl sulfide on the enhanced substrate. (c) Headspace SERS spectra of the time-dependent adsorption from BHI broth spiked with 1×10^{-2} m DMDS. A total of 24 spectra recorded at 15 min intervals with Ag substrate. (d and e) Growth of SERS signal over time for methyl sulfide in BHI broth supplemented with different concentrations of DMDS with Ag substrate. (f–g) SERS spectra from *Escherichia coli* culture on (f) Ag and (g) Au substrates. (h and i) Comparison of kinetic data of bacterial growth (OD) with time for increasing intensity of methyl sulfide SERS with (h) Ag and (i) Au as substrates. *Source*: Reproduced from Kelly et al. (2018) with permission from Wiley Online Library, copyright 2018.

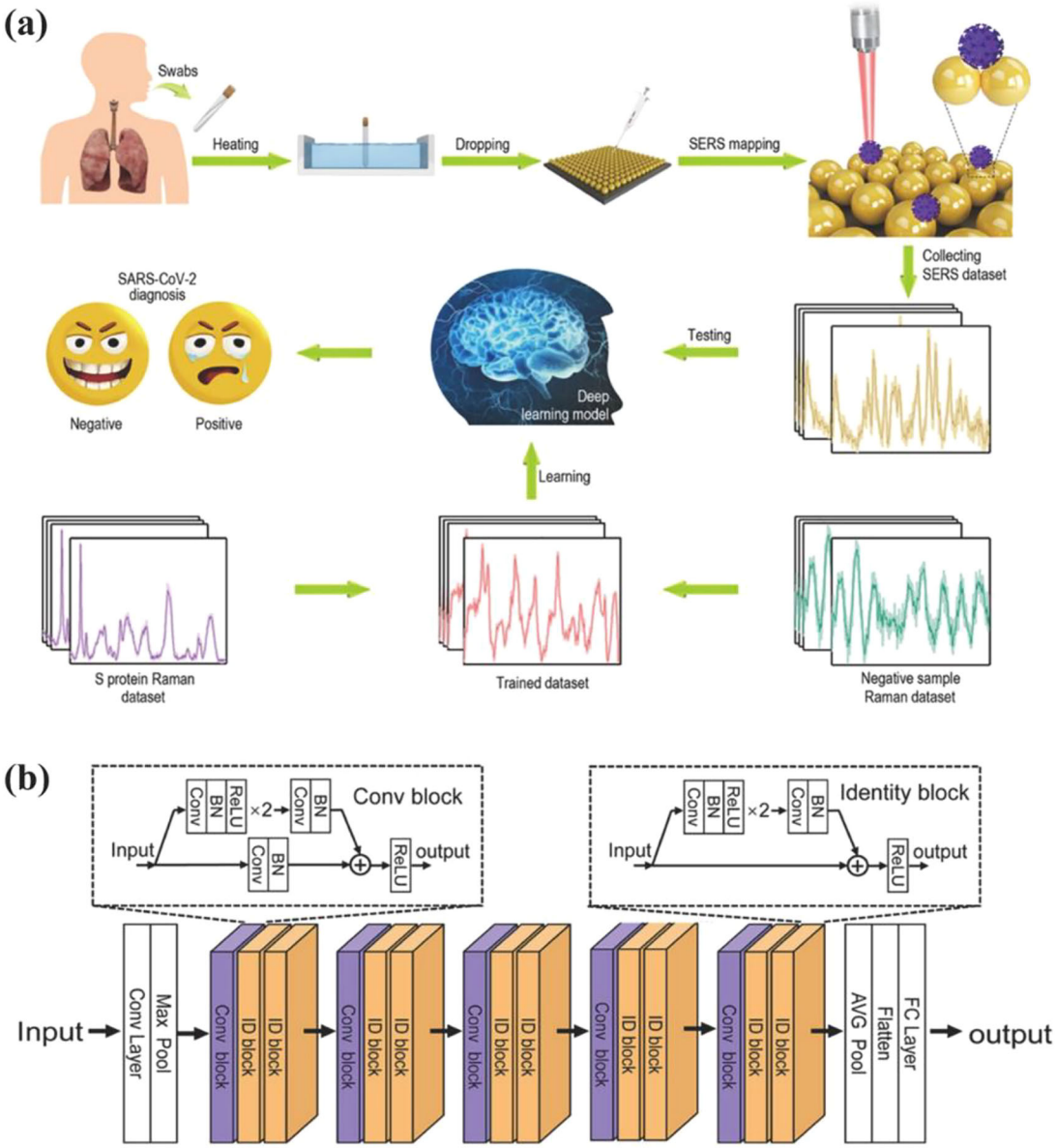

FIGURE 6 (a) The overview of process using deep learning–based surface-enhanced Raman spectroscopy (SERS) approach for the detection of the coronavirus disease (COVID-19). (b) The flowchart of the deep learning model based on residual neural networks for the detection of severe acute respiratory syndrome coronavirus 2 (SARS-CoV-2). *Source*: Adapted from Huang et al. (2021) with permission from ACS Publications, copyright 2021.

of viral structure at the molecular scale, providing researchers with timely information on SARS-CoV-2 mutations and their subtypes.

Raman spectroscopy enables the characterization of nucleic acids and proteins of viral contaminants, without requiring any treatment. Earlier research has focused on examining viral RNA, DNA, and proteins using Raman spectra (Thomas, 1976). These investigations underscore the extraordinary advantages of dispersive Raman spectroscopy methods. The combination of different excitation wavelengths and Raman microscope in the dispersive Raman system has facilitated the examination of multiple pathogenic viruses. However, as an organism with a more straightforward structure than other microorganisms, most viruses share similar structures. Thus, the Raman signals acquired by these systems typically exhibit resemblances, and detecting their differences is difficult. In addition to the necessary statistical analysis, indirect viral analysis can be performed by detecting surrogates or reporter molecules instead of viruses. Typically, these techniques involve the physical coupling of the virus and the reporter to create a nanotag.

Adenoviruses are double-stranded DNA viruses without envelopes. They may cause acute respiratory disease, pneumonia, acute follicular conjunctivitis, cystitis, and gastroenteritis (Doerfler, 1996). Moor et al. (2018) achieved the early detection of viral infection in live human cells using Raman techniques. In this study, the viral vector Ad-CMV-control

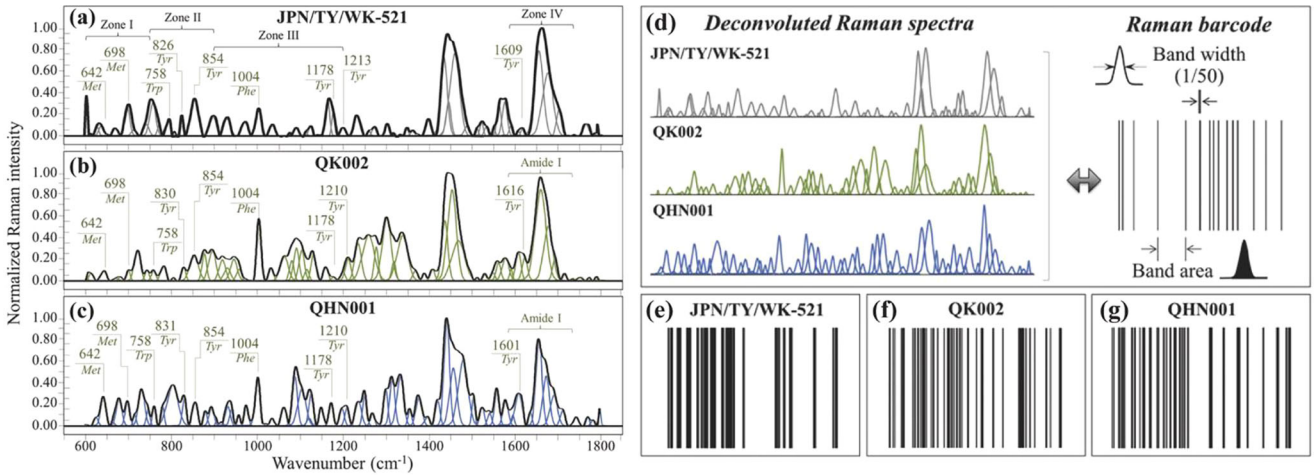

FIGURE 7 (a–c) Raman spectra in the frequency interval 600–1800 cm^{-1} of the (a) original Japanese isolate JPN/TY/WK-521, (b) variant QK002, and (c) variant QHN001. Labels demonstrate frequencies at the maximum of selected bands (Met, Tyr, and Phe are abbreviations for methionine, tyrosine, and phenylalanine, respectively). (d) The sequence of Raman Gauss–Lorentz bands deconvoluted from the average Raman spectra of the original Japanese isolate and two UK variants (see labels), and an algorithm to convert the band sequences into barcodes. (e–g) Barcodes constructed for the sub-band sequences in (a). *Source*: Adapted from Pezzotti et al. (2022) with permission from Wiley Online Library, copyright 2022.

(AdC), which lacks the E1 gene coding for an early polypeptide, was used as the target virus, and human embryonic kidney 293 cells were introduced to possess the E1 gene, which contains the promoter of the E2 gene for a DNA polymerase that is specific to replication of the viral genome. The E2 peptide characteristic peaks indicated that the E2 gene was quickly transferred into the nucleus after virus invasion. This study established that the detection threshold for SERS can be reduced to a single molecule.

Similarly, this alternative diagnostic platform using SERS nanotags has been widely applied to other types of viruses. For example, the Ebola virus has been known to cause a significant epidemic in African countries in recent years. In several studies, Sebba et al. have proposed a particle-based sandwich immunoassay to detect and differentiate infections with Ebola from other more common febrile diseases (malaria and Lassa fever virus). Sebba et al. (2018) created a stable optical signal by encapsulating the SERS-active Raman reporter between a 60nm AuNP, which acts as the nanotag core, instead of attempting to detect proteins directly using SERS signals. This prospective study achieved 90.0% and 100.0% sensitivities and 97.9% and 99.6% specificities for the Ebola virus and malaria, respectively, in blood samples from non-primate animals, indicating the potential of SERS technology as an essential tool for clinical triage in low-resource settings. Recently, more evidence has demonstrated the wide range of prospects of Raman techniques for detecting viral infections, especially regarding cross-species viruses, such as the avian influenza virus (Neng et al., 2018) and Rift Valley fever virus (Shiratori et al., 2014; Xiao et al., 2019). These outstanding achievements will break the limits of laboratory resources, circumvent the requirement for dedicated personnel, and make an exceptional contribution to the future of epidemiological testing.

3.3 | Neurological diseases

Neurodegenerative diseases are a group of conditions in which neurons of the brain and spinal cord lose their function (Dugger & Dickson, 2017), and dementia is one of the most common features of these diseases. Currently, approximately 50 million people have dementia (Nichols et al., 2019), which is estimated to increase to 130 million by 2050 (Prince et al., 2015). Additionally, this group of diseases has no viable treatment, although early intervention may help delay the development process. Furthermore, previous studies have reported that relevant polymorphs accumulate in the brain tissue 10–30 years before the onset of dementia (Gordon et al., 2018). Therefore, the pre-onset detection of disease trends may be a direction for future clinical diagnosis.

3.3.1 | Alzheimer's disease

AD is the most prevalent neurodegenerative disease, affecting millions of patients worldwide, with a continuously increasing incidence (Prince et al., 2015). Although the pathogenesis of AD remains controversial, several polymers in the cerebrospinal fluid and blood have been proven to be associated with the disease. These include neurofilament light chain, neuron-specific enolase, heart fatty acid–binding protein, chitinase-3-like protein 1, and visinin-like protein 1 (Gordon et al., 2018). As AD is often detected after irreversible brain damage has occurred, and the definitive diagnosis can only be achieved post-mortem based on the detection and identification of the aggregates, the development of a sensitive and affordable diagnostic approach for AD represents a significant challenge in the field.

Among many spectral analysis tools, Raman spectroscopy demonstrates high potential for identifying early-stage AD and its differentiation from late forms of the disease (Paraskevaidi et al., 2018; Ryzhikova et al., 2021), as it is well suited for analyzing water-containing samples. However, the development of Raman techniques as diagnostic tools is challenging. First, the Raman signals of biomolecules are generally weak, and frequent fluorescence interference hinders the promotion of new technological breakthroughs. Several signal enhancement techniques have been used to overcome these limitations, including SERS (Carlomagno et al., 2020; Cennamo et al., 2020), TERS (Tabata, 2017; Zikic et al., 2021), CARS (Talaga et al., 2018), and SRS (Cunha et al., 2021; Ji et al., 2018). These optimized Raman-related diagnostic techniques have been commonly used in the latest prospective studies for detecting different samples.

As previously stated, blood and cerebrospinal fluid are the most frequently analyzed samples, as they may be the most biologically significant body fluids for AD. For example, Ryzhikova et al. (2021) explored the potential of combining ML with Raman spectroscopy to differentiate between CSF samples obtained from patients with AD and healthy controls. They explained the reasons for the characteristic bands associated with amino acid metabolism. This study achieved acceptable accuracy (84%), but its specific efficiency was further validated owing to the small sample size. Similarly, based on the classification of patients with AD and healthy individuals, Paraskevaidi et al. (2018) attempted to differentiate the biochemical composition of the blood plasma of early-stage AD, late-stage AD, and patients with dementia with Lewy bodies (Figure 8). The achievement of AD staging and differentiation between the two dementias may indicate that some future uses of Raman techniques could be used to detect prodromal or prognostic cases for early appropriate medical interventions.

Several studies have also been dedicated to determining the correlation between neurotoxicity and the structural characteristics of various forms of $A\beta_{42}$ (Banchelli et al., 2019, 2020). Banchelli et al. (2020) inspected the outermost layers of $A\beta$ species to detect distinctive structural motifs associated with toxic forms using SERS coupled with an intertwined silver nanowire (AgNW)-based platform. They summarized the chemical structural differences between cytotoxic $A\beta_{42}$ (A+ oligomers) and noncytotoxic forms of $A\beta_{42}$ (A− oligomers). The authors established a connection between the exposure of Tyr and Lys residues and the toxicity of $A\beta_{42}$ oligomers (Figure 9). Moreover, SERS was employed to examine the secondary structures of various amyloid-β peptides, enabling the elucidation of structural rearrangement processes through Raman signals. This contributes to clarifying the mechanism of AD (Tabata, 2017; Zikic et al., 2021; Garcia-Leis & Sanchez-Cortes, 2021).

These studies demonstrate the potential of Raman techniques for enabling early AD diagnosis. However, recent studies have explored the earlier stages of self-aggregation and fibrillation (Zikic et al., 2021; Garcia-Leis & Sanchez-Cortes, 2021). All of these studies constitute a complete, full-stage diagnostic system that will elucidate the pathogenesis of AD in the future and benefit patients.

3.3.2 | Parkinson's disease

Parkinson's disease (PD) ranks as the second most significant neurodegenerative disorder after AD, with an increasing burden on an aging society (Berg, 2008). Like AD, PD also results from the degeneration and loss of function of neurons in the brain and peripheral nervous system. It is often diagnosed through the presence of neuritic plaques and α-synuclein, which is considered the most promising biomarker. Therefore, many Raman-based studies have been conducted to explore this biomarker. Carlomagno et al. (2021a) reported an ML-assisted Raman spectroscopy approach to identify the Raman Salivary fingerprint of PD. Global Raman signals were collected from the saliva of 23 PD patients, associated healthy and pathological control groups. Subsequently, machine and deep learning methods were used to compute and create a classification model based on the obtained Raman spectra. As a result, this model can distinguish each spectrum with specificity, accuracy, and sensitivity of higher than 97%. Furthermore, the data were greatly correlated with clinical data for the PD diagnosis and monitoring utilized nowadays. However, given that only 23 PD patients' data were obtained and summarized in this study. Larger cohorts are needed to validate this approach. Similarly, another study has proposed a model based on Raman signals with three different types of neurodegenerative symptoms (PD, AD, and mild cognitive impairment) (Ryzhikova et al., 2015). The differences among each group were statistically significant, and those among samples in the same group can be explained by drug treatment, inspiring both the differentiation of neurodegenerative diseases and the exploration of the optimal dosage of medication.

Moreover, some early studies have confirmed that α-synuclein might reduce dopamine levels in the blood of patients with PD by mediating selective deletion of dopaminergic neurons (Masliah et al., 2000; Vila et al., 2000). Therefore, L-dopa and dopamine-receptor agonists are often used to improve dopamine deficiency in the serum for the treatment of PD (Dunn et al., 2017; Olanow et al., 2000). This advancement has greatly inspired the use of Raman technology to investigate dopamine as a biomarker for diagnosing PD, including concentration measurement (Cutler, 2019) and exploration of adsorption mechanisms (Figueir, 2020). Other studies have attempted to detect and image dopamine in the presence of interfering species in animal models (Figueir, 2020). Ren et al. (2021) presented a dopamine-imaging methodology based on SERS in the cells and retinal tissues of guinea pigs and mouse models (Figure 10). The functionalized AuNP probes were citrate-capped with a diameter of 40 nm, which were surface-modified and stabilized using a combination of three thiolated molecules: *N*-butylboronic acid-2-mercaptoethylamine, *N*-hydroxysuccinimide ester, and 3-sulfanylpropanenitrile. These molecules selectively reacted with the two hydroxyl groups and amine group of dopamine, respectively (Figure 10a). Dopamine triggered the aggregation of AuNPs, resulting in the formation of plasmonic hotspots that significantly amplified Raman signals.

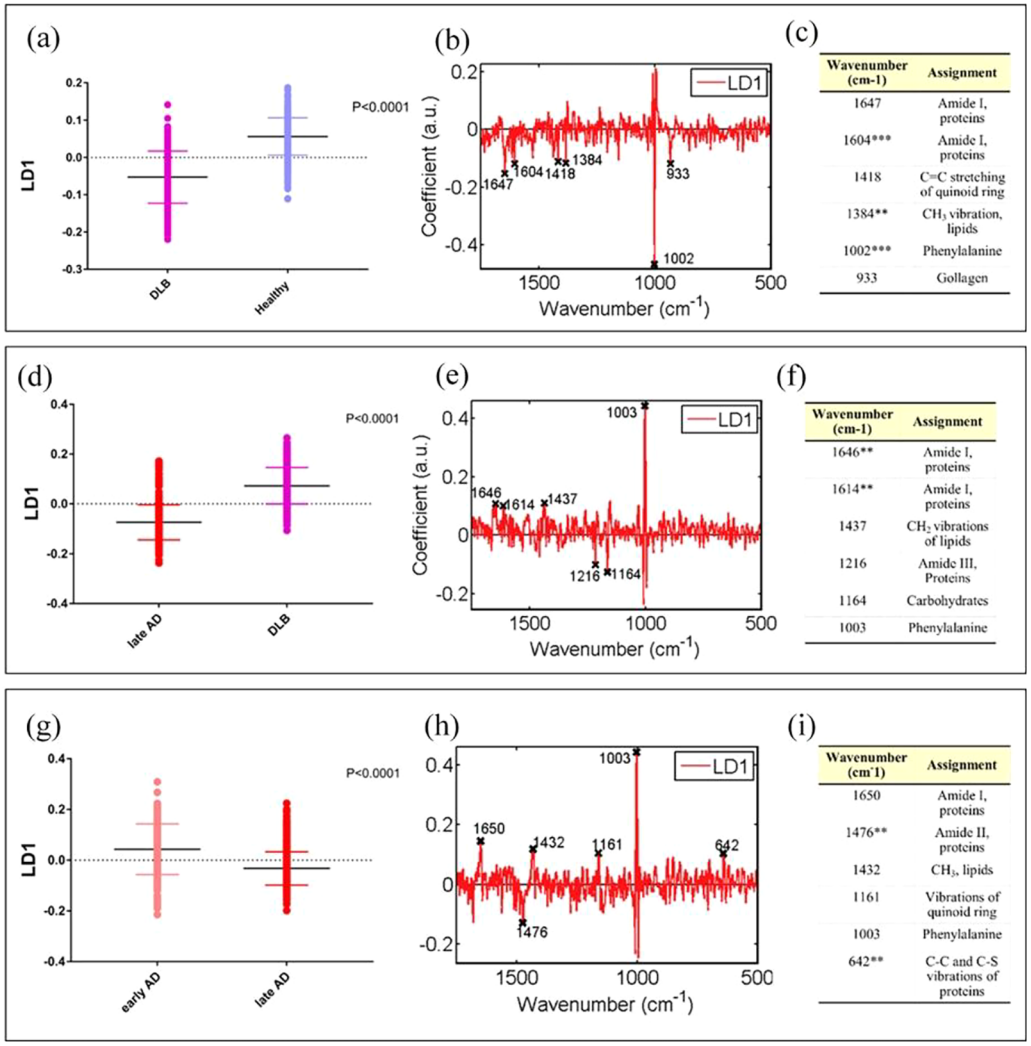

FIGURE 8 One-dimensional (1D) scores plot after cross-validated principal component analysis, linear discriminant analysis (PCA–LDA) ($p < .0001$, 95% CI = .138–.1596) of early-stage Alzheimer's disease (AD) versus dementia with Lewy bodies (DLB) (a–c), late-stage AD versus DLB (d–f), and early-stage AD compared with late AD (g–i). Loading plot indicates the top six discriminatory peaks (left column), important peaks along with their tentative assignments (middle column), and the mean ± standard deviation ($p \leq .05$ was considered significant; $p < .05$, <.005, and <.0005 were shown by *, **, and ***, respectively (right column). *Source*: Reproduced from Paraskevaidi et al. (2018) with permission from ACS Publications, copyright 2018.

As presented in Figure 10, the detection limit was measured by introducing different concentrations of dopamine (ranging from 0 to 10 μM) to the functionalized AuNPs. The color of the functionalized AuNPs underwent a progressive transition from wine red to purple, correlating with the concentration of dopamine and indicating particle aggregation. This aggregation was further validated through transmission electron microscopy analysis (Figure 10c). The UV–vis spectra exhibited a consistent pattern with the observed color variations. The SERS spectra were similar to those of the colorimetric assay (Figure 10d). This prospective study at the cellular level provides potential for further in vivo testing of dopamine, taking into consideration factors such as cytotoxicity of AuNPs and laser safety.

4 | CHALLENGES, OUTLOOK, AND CONCLUSION

The robustness of Raman scattering–based techniques lies in their ability to perform label-free and highly sensitive analysis of biomolecules, making them valuable tools for clinical diagnosis. Despite some challenges, the strength of Raman scattering will lead to the development of applications with a broader diagnostic scope, covering more lesions of different tissues. We anticipate several promising directions in the future. First, the lesion process is often accompanied by many complex biochemical reactions; however, current studies have clarified only a few reactions. In such cases, more specific molecular markers should be identified for different lesions in human tissue samples, and

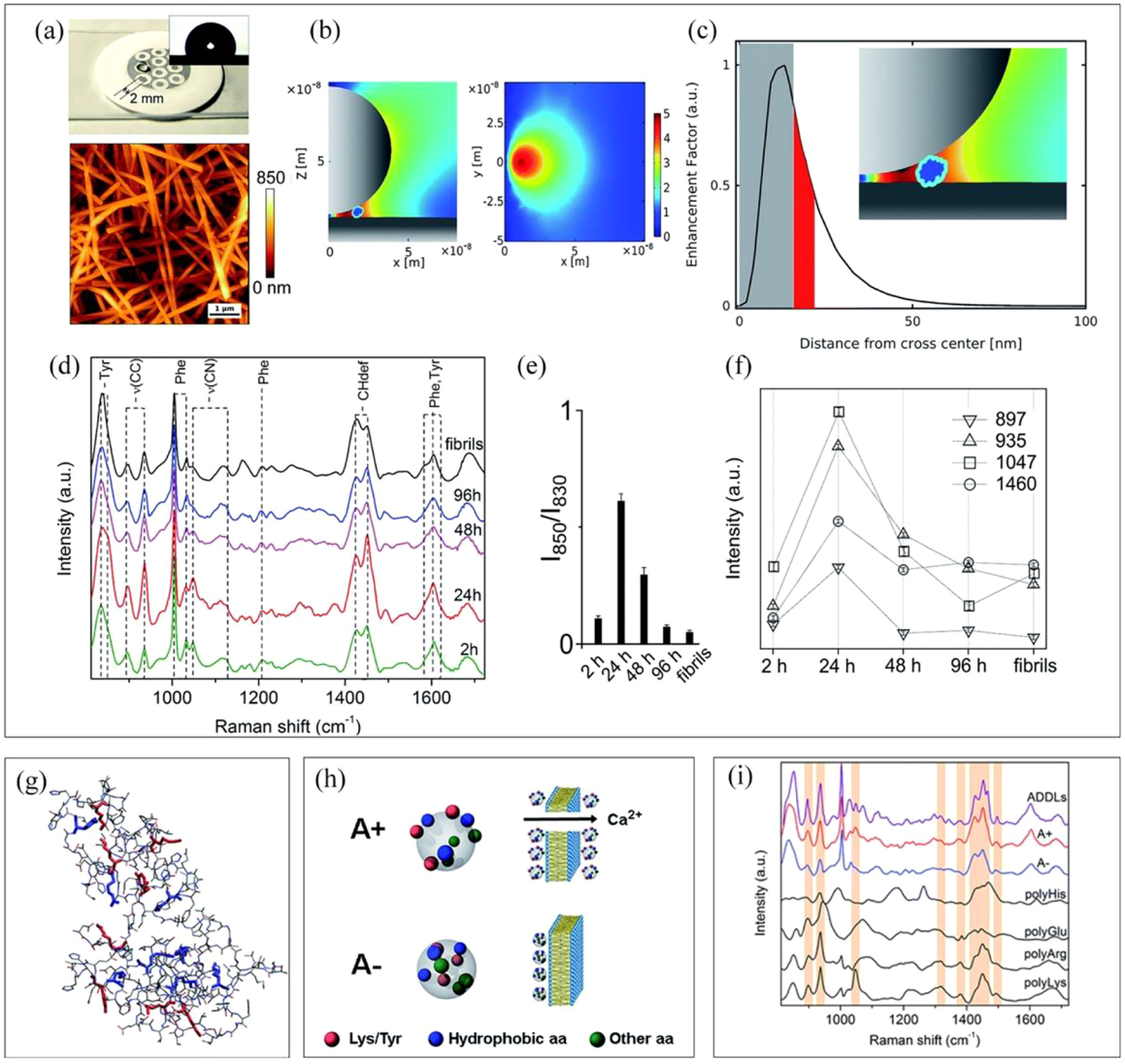

FIGURE 9 Surface-enhanced Raman spectroscopy (SERS) analysis of Aβ_{42} species. (a) Silver spot substrate used for SERS analysis, showing a drop of Aβ_{42} solution deposited on a 2 mm large spot. (b) 2D sections *xz* on the left and *xy* on the right of finite element method (FEM) simulations of the *E*-field intensity ($|E|/|E0|$) in-between two crossed AgNWs in air. (c) Profile of EF along the *x*-direction. The gray region adjacent to the origin of the intersection (from 0 to ~15 nm) is denied to the oligomer due to steric impediments, whereas the zone highlighted in red indicates the enhancement factor. (d) Series of SERS spectra of Aβ_{42} oligomers over different incubation times and of mature fibrils (from bottom to top) in the range 800–1750 of cm^{-1}, characteristic bands are marked with dashed lines. (e) The ratio of 850 and 830 cm^{-1} band intensities of Tyr doublet. (f) The integrated area values of bands from spectra in (d). (g) Representative structure of compact ($R < .9$) Aβ_{42} oligomer. (h) Schematic representation of the A+ and A− oligomers of Aβ42. Toxic A+ oligomers are characterized by the exposure of hydrophobic clusters (blue), and Tyr and Lys residues (red). (i) SERS spectra of ADDLS, type A+ and A− oligomers, polyHis, PolyGlu, PolyArg, and PolyLys, respectively. The bands of polyLys and/or polyArg indicating the spectral properties associated with A+ oligomers and ADDLs are marked with color boxes. *Source*: Reproduced from Banchelli et al. (2020) with permission from Royal Society of Chemistry, copyright 2020.

the relationships between markers and certain diseases need to be established. Second, as with most spectroscopic techniques, Raman spectroscopy requires advanced data processing to extract meaningful information from spectra. ML has provided an unprecedented opportunity to extract information from complex or extensive spectroscopic datasets. However, the performance of ML models is highly dependent on the quality of the features fed into the model for classification, which implies that ML requires extensive feature extraction and selection when processing large-scale data. As spectroscopy advances and spectral datasets increase, deep learning, which has achieved autonomous feature extraction, will be the focus of research on spectral processing methods. Additionally, most existing studies have been performed using known lesion samples and normal samples to make the distinction, although when Raman technology becomes a common tool for clinical diagnosis, the parameters associated with pathological diagnosis need to be standardized.

Research on the applications of Raman spectroscopy in clinical medicine is critical because it has the potential to revolutionize

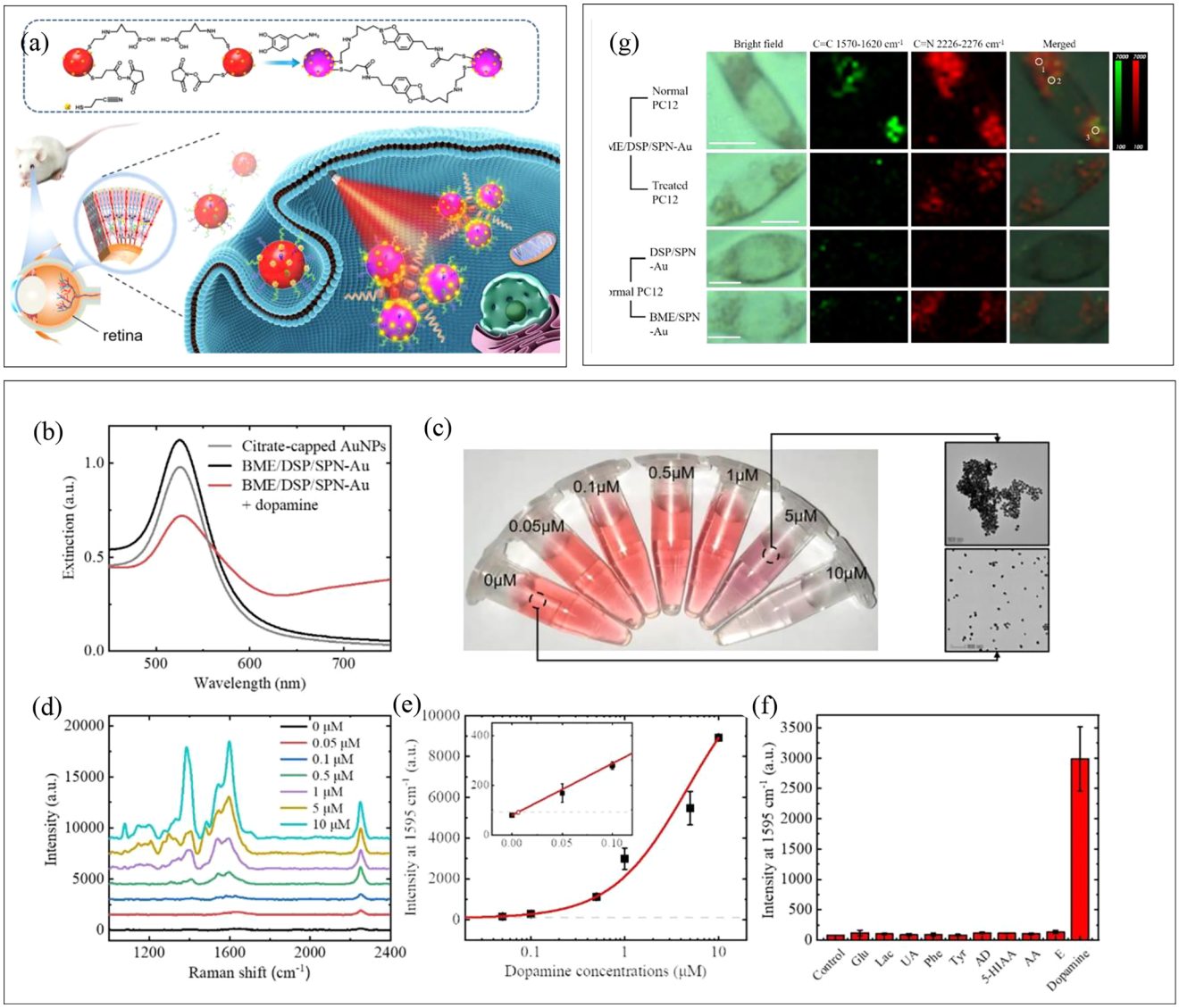

FIGURE 10 (a) Overview of surface-enhanced Raman spectroscopy (SERS) detection based on functional gold nanoparticles (AuNPs) for local dopamine imaging. (b–f) Characterization of dopamine detection using BME/DSP/SPN-Au probes:(b) UV–vis spectra of the citrate-capped AuNPs (gray), before (black), and after (red) addition of dopamine to functionalized BME/DSP/SPN-Au probes. (c) Nanoprobes after adding 0–10 μM of dopamine. (d) SERS spectra of nanoprobes after the addition of different concentrations of dopamine. (e) The relationship between the intensity at 1595 cm^{-1} and the different concentrations of dopamine. (f) Histogram of Raman intensities at 1595 cm^{-1} in the presence of 1 μM different substances. (g) The bright field, SERS images, and their merged images of differently treated single living cells obtained in 1570–1620 and 2226–2276 cm^{-1} channels under different treatments. *Source*: Reproduced from Ren et al. (2021) with permission from ACS Publications, copyright 2021.

healthcare by providing a noninvasive, rapid, and accurate diagnostic tool for various diseases, including cancers, infections, and neurodegenerative diseases. In this article, we provided a comprehensive overview on the applications of Raman spectroscopy in the area of biomedical sciences. We introduced current methods of applying Raman in ex vivo and in vivo detection and Raman acquisition enhancement techniques. Moreover, the applications of Raman in cancer and precancerous lesions, infectious diseases, and neurological diseases have been reviewed and discussed. Finally, we present the challenges of the existing research and provide valuable perspectives on potential future advancements in the application of Raman spectroscopy in the field of biomedical sciences. However, oxidative stress processes might precede or indicate the pre-installation of pathological/neurodegenerative or oncological conditions. Their role in the interpretation of clinically relevant band assignments and specific biomarkers observed from the Raman/SERS spectra must be considered. This is because the spectral bands are also relevant in the diagnosis decision, as part of the malignant/critical conditions is pre-signalized by inflammatory processes. Therefore, a comprehensive analysis of the spectral data is necessary when applying Raman/SERS-based methodology to clinical samples. For example, how is stage diagnosis affected by oxidative

stress processes, and is the diagnosis decision made considering such processes?

SERS faces other challenges as well. For instance, in order for SERS to be used in vivo, it is essential to address the issues of biocompatibility and toxicity. Current researchers are developing biocompatible NPs or substrates that minimize adverse effects on living tissues. Furthermore, studies are being conducted to assess the long-term effects and potential toxicity of SERS probes in vivo. Additionally, SERS encounters reproducibility issues that are influenced by the substrate used. Researchers are developing standardized protocols for substrate fabrication to ensure reproducible and consistent results. They are also searching for new substrate materials and surface modifications to improve reliability and reproducibility. Additionally, for the application of Raman spectroscopy in in vivo tissue or disease screening, its clinical translation is hindered by factors such as laser safety. This is because in vivo Raman spectroscopy often requires high power or long integration times to overcome the intrinsically weak Raman signal. Researchers are currently developing approaches to optimize laser parameters, including wavelength and power, in order to minimize tissue damage while maintaining an adequate SNR. They are also exploring new laser sources and delivery systems that can provide safer and more efficient excitation. Therefore, further advancements in the application of Raman spectroscopy in biomedical sciences are expected in the near future.

AUTHOR CONTRIBUTIONS

Yaping Qi, Yucheng Jiang, Zi Chen, and Yong P. Chen performed conceptualization, funding acquisition, supervision, writing—original draft, writing—reviewing and editing. Esther Xinyi Chen, Dan Hu, Ying Yang, Zhenping Wu, Ming Zheng, Mohammad A. Sadi, and Kang Zhang wrote along with reviewing and editing.

ACKNOWLEDGMENTS

We acknowledge the support of this work by the Macau Science and Technology Development Fund (FDCT Grants 0031/2021/ITP). We also acknowledge the support of Tohoku University and WPI-AIMR, and Purdue University Discovery Park Big Idea Challenge program.

CONFLICT OF INTEREST STATEMENT

The authors declare no conflicts of interest.

ORCID

Yaping Qi https://orcid.org/0000-0002-0367-3695

REFERENCES

Abramczyk, H., & Brozek-Pluska, B. (2013). Raman imaging in biochemical and biomedical applications. Diagnosis and treatment of breast cancer. *Chemical Reviews*, *113*(8), 5766–5781.

Albrecht, A. C. (1961). On the theory of Raman intensities. *Journal of Chemical Physics*, *34*(5), 1476.

Ali, S. M., Bonnier, F., Tfayli, A., Lambkin, H., Flynn, K., Mcdonagh, V., Healy, C., Clive Lee, T., Lyng, F. M., & Byrne, H. J. (2013). Raman spectroscopic analysis of human skin tissue sections ex-vivo: Evaluation of the effects of tissue processing and dewaxing. *Journal of Biomedical Optics*, *18*(6), 061202.

Aljakouch, K., Hilal, Z., Daho, I., Schuler, M., Krauß, S. D., Yosef, H. K., Dierks, J., Mosig, A., Gerwert, K., & El-Mashtoly, S. F. (2019). Fast and noninvasive diagnosis of cervical cancer by coherent anti-stokes Raman scattering. *Analytical Chemistry*, *91*(21), 13900–13906.

Almond, L. M., Hutchings, J., Lloyd, G., Barr, H., Shepherd, N., Day, J., Stevens, O., Sanders, S., Wadley, M., Stone, N., & Kendall, C. (2014). Endoscopic Raman spectroscopy enables objective diagnosis of dysplasia in Barrett's esophagus. *Gastrointestinal Endoscopy*, *79*(1), 37–45.

Areia, M., Amaro, P., Dinis-Ribeiro, M., Cipriano, M. A., Marinho, C., Costa-Pereira, A., Lopes, C., Moreira-Dias, L., Romãozinho, J. M., Gouveia, H., Freitas, D., & Leitão, M. C. (2008). External validation of a classification for methylene blue magnification chromoendoscopy in premalignant gastric lesions. *Gastrointestinal Endoscopy*, *67*(7), 1011–1018.

Asai, N., Motojima, S., Ohkuni, Y., Matsunuma, R., Nakashima, K., Iwasaki, T., Nakashita, T., Kaneko, N., & Otsuka, Y. (2012). Early diagnosis and treatment are crucial for the survival of *Pneumocystis* pneumonia patients without human immunodeficiency virus infection. *Journal of Infection and Chemotherapy*, *18*(6), 898–905.

Ashton, L., Lau, K., Winder, C. L., & Goodacre, R. (2011). Raman spectroscopy: Lighting up the future of microbial identification. *Future Microbiology*, *6*(9), 991–997.

Avella-Oliver, M., Puchades, R., Wachsmann-Hogiu, S., & Maquieira, A. (2017). Label-free SERS analysis of proteins and exosomes with large-scale substrates from recordable compact disks. *Sensors and Actuators B: Chemical*, *252*, 657–662.

Azzi, L., Carcano, G., Gianfagna, F., Grossi, P., Gasperina, D. D., Genoni, A., Fasano, M., Sessa, F., Tettamanti, L., Carinci, F., Maurino, V., Rossi, A., Tagliabue, A., & Baj, A. (2020). Saliva is a reliable tool to detect SARS-CoV-2. *Journal of Infection*, *81*(1), e45–e50.

Banchelli, M., Amicucci, C., Ruggiero, E., D'andrea, C., Cottat, M., Ciofini, D., Osticioli, I., Ghini, G., Siano, S., Pini, R., De Angelis, M., & Matteini, P. (2019). Spot-on SERS detection of biomolecules with laser-patterned dot arrays of assembled silver nanowires. *ChemNanoMat*, *5*(8), 1036.

Banchelli, M., Cascella, R., D'andrea, C., Cabaj, L., Osticioli, I., Ciofini, D., Li, M. S., Skupień, K., De Angelis, M., Siano, S., Cecchi, C., Pini, R., La Penna, G., Chiti, F., & Matteini, P. (2020). Nanoscopic insights into the surface conformation of neurotoxic amyloid β oligomers. *RSC Advances*, *10*(37), 21907–21913.

Barroso, E. M., Smits, R. W. H., Van Lanschot, C. G. F., Caspers, P. J., Ten Hove, I., Mast, H., Sewnaik, A., Hardillo, J. A., Meeuwis, C. A., Verdijk, R., Noordhoek Hegt, V., Baatenburg De Jong, R. J., Wolvius, E. B., Bakker Schut, T. C., Koljenović, S., & Puppels, G. J. (2016). Water concentration analysis by Raman spectroscopy to determine the location of the tumor border in oral cancer surgery. *Cancer Research*, *76*(20), 5945–5953.

Barta, J. A., Powell, C. A., & Wisnivesky, J. P. (2019). Global epidemiology of lung cancer. *Annals of Global Health*, *85*(1), 8.

Bearman, G. M. L., & Wenzel, R. P. (2005). Bacteremias: A leading cause of death. *Archives of Medical Research*, *36*(6), 646–659.

Berg, D. (2008). Biomarkers for the early detection of Parkinson's and Alzheimer's disease. *Neurodegenerative Diseases*, *5*, 133–136.

Bergholt, M. S., Zheng, W., Ho, K. Y., Teh, M., Yeoh, K. G., Yan So, J. B., Shabbir, A., & Huang, Z. (2014). Fiberoptic confocal Raman spectroscopy for real-time in vivo diagnosis of dysplasia in Barrett's esophagus. *Gastroenterology*, *146*(1), 27–32.

Bergholt, M. S., Zheng, W., Lin, K., Ho, K. Y., Teh, M., Yeoh, K. G., So, J. B. Y., & Huang, Z. (2011). In vivo diagnosis of esophageal cancer using image-guided Raman endoscopy and biomolecular modeling. *Technology in Cancer Research & Treatment*, *10*(2), 103–112.

Birech, Z., Mwangi, P. W., Bukachi, F., & Mandela, K. M. (2017). Application of Raman spectroscopy in type 2 diabetes screening in blood using leucine and isoleucine amino-acids as biomarkers and in comparative anti-diabetic drugs efficacy studies. *PLoS ONE*, *12*, e0185130.

Birech, Z., Ondieki, A. M., Opati, R. I. I., & Mwangi, P. W. (2020). Low cost Raman sample substrates from conductive silver paint smear for Raman spectroscopic screening of metabolic diseases in whole blood. *Vibrational Spectroscopy*, *108*, 103063.

Blake, N., Gaifulina, R., Griffin, L. D., Bell, I. M., & Thomas, G. M. H. (2022). Machine learning of Raman spectroscopy data for classifying cancers: A review of the recent literature. *Diagnostics (Basel)*, *12*(6), 1491.

Bonhommeau, S., Cooney, G. S., & Huang, Y. (2022). Nanoscale chemical characterization of biomolecules using tip-enhanced Raman spectroscopy. *Chemical Society Reviews*, *51*(7), 2416–2430.

Bonifacio, A., Cervo, S., & Sergo, V. (2015). Label-free surface-enhanced Raman spectroscopy of biofluids: Fundamental aspects and diagnostic applications. *Analytical and Bioanalytical Chemistry*, *407*(27), 8265–8277.

Bovenkamp, D., Sentosa, R., Rank, E., Erkkilä, M., Placzek, F., Püls, J., Drexler, W., Leitgeb, R., Garstka, N., Shariat, S., Stiebing, C., Schie, I., Popp, J., Andreana, M., & Unterhuber, A. (2018). Combination of high-resolution optical coherence tomography and Raman spectroscopy for improved staging and grading in bladder cancer. *Applied Sciences*, *8*, 2371.

Bratchenko, L. A., Bratchenko, I. A., Lykina, A. A., Komarova, M. V., Artemyev, D. N., Myakinin, O. O., Moryatov, A. A., Davydkin, I. L., Kozlov, S. V., & Zakharov, V. P. (2019). Comparative study of multivariative analysis methods of blood Raman spectra classification. *Journal of Raman Spectroscopy*, *51*(2), 14.

Brenner, H., Arndt, V., Stürmer, T., Stegmaier, C., Ziegler, H., & Dhom, G. (2001). Long-lasting reduction of risk of colorectal cancer following screening endoscopy. *British Journal of Cancer*, *85*(7), 972–976.

Brozek-Pluska, B., Kopec, M., Surmacki, J., & Abramczyk, H. (2018). Histochemical analysis of human breast tissue samples by IR and Raman spectroscopies. Protocols discussion. *Infrared Physics & Technology*, *93*, 247–254.

Bukva, M., Dobra, G., Gomez-Perez, J., Koos, K., Harmati, M., Gyukity-Sebestyen, E., Biro, T., Jenei, A., Kormondi, S., Horvath, P., Konya, Z., Klekner, A., & Buzas, K. (2021). Raman spectral signatures of serum-derived extracellular vesicle-enriched isolates may support the diagnosis of CNS tumors. *Cancers (Basel)*, *13*(6), 1407.

Bury, D., Morais, C. L. M., Ashton, K. M., Dawson, T. P., & Martin, F. L. (2019). Ex vivo Raman spectrochemical analysis using a handheld probe demonstrates high predictive capability of brain tumour status. *Biosensors (Basel)*, *9*(2), 49.

Butler, H. J., Ashton, L., Bird, B., Cinque, G., Curtis, K., Dorney, J., Esmonde-White, K., Fullwood, N. J., Gardner, B., Martin-Hirsch, P. L., Walsh, M. J., Mcainsh, M. R., Stone, N., & Martin, F. L. (2016). Using Raman spectroscopy to characterize biological materials. *Nature Protocols*, *11*(4), 664–687.

Carlomagno, C., Bertazioli, D., Gualerzi, A., Picciolini, S., Andrico, M., Rodà, F., Meloni, M., Banfi, P. I., Verde, F., Ticozzi, N., Silani, V., Messina, E., & Bedoni, M. (2021). Identification of the Raman salivary fingerprint of Parkinson's disease through the spectroscopic-computational combinatory approach. *Frontiers in Neuroscience*, *15*, 704963.

Carlomagno, C., Bertazioli, D., Gualerzi, A., Picciolini, S., Banfi, P. I., Lax, A., Messina, E., Navarro, J., Bianchi, L., Caronni, A., Marenco, F., Monteleone, S., Arienti, C., & Bedoni, M. (2021). COVID-19 salivary Raman fingerprint: Innovative approach for the detection of current and past SARS-CoV-2 infections. *Scientific Reports*, *11*(1), 4943.

Carlomagno, C., Cabinio, M., Picciolini, S., Gualerzi, A., Baglio, F., & Bedoni, M. (2020). SERS-based biosensor for Alzheimer disease evaluation through the fast analysis of human serum. *Journal of Biophotonics*, *13*(3), e201960033.

Carrola, J., Rocha, C. M., Barros, A. S., Gil, A. M., Goodfellow, B. J., Carreira, I. M., Bernardo, J., Gomes, A., Sousa, V., Carvalho, L., & Duarte, I. F. (2011). Metabolic signatures of lung cancer in biofluids: NMR-based metabonomics of urine. *Journal of Proteome Research*, *10*(1), 221–230.

Cennamo, G., Montorio, D., Morra, V. B., Criscuolo, C., Lanzillo, R., Salvatore, E., Camerlingo, C., Lisitskiy, M., Delfino, I., Portaccio, M., & Lepore, M. (2020). Surface-enhanced Raman spectroscopy of tears: Toward a diagnostic tool for neurodegenerative disease identification. *Journal of Biomedical Optics*, *25*(8), 1–12.

Chen, F., Sun, C., Yue, Z., Zhang, Y., Xu, W., Shabbir, S., Zou, L., Lu, W., Wang, W., Xie, Z., Zhou, L., Lu, Y., & Yu, J. (2022). Screening ovarian cancers with Raman spectroscopy of blood plasma coupled with machine learning data processing. *Spectrochimica Acta. Part A, Molecular and Biomolecular Spectroscopy*, *265*, 120355.

Choi, S., Moon, S. W., Shin, J.-H., Park, H.-K., & Jin, K.-H. (2014). Label-free biochemical analytic method for the early detection of adenoviral conjunctivitis using human tear biofluids. *Analytical Chemistry*, *86*(22), 11093–11099.

Choo-Smith, L.-P., Edwards, H. G. M., Endtz, H. P., Kros, J. M., Heule, F., Barr, H., Robinson, J. S., Bruining, H. A., & Puppels, G. J. (2002). Medical applications of Raman spectroscopy: From proof of principle to clinical implementation. *Biopolymers: Original Research on Biomolecules*, *67*(1), 1–9.

Cialla-May, D., Zheng, X.-S., Weber, K., & Popp, J. (2017). Recent progress in surface-enhanced Raman spectroscopy for biological and biomedical applications: From cells to clinics. *Chemical Society Reviews*, *46*(13), 3945–3961.

Cucinotta, D., & Vanelli, M. (2020). WHO declares COVID-19 a pandemic. *Acta Biomedica: Atenei Parmensis*, *91*, 157–160.

Cui, L., Butler, H. J., Martin-Hirsch, P. L., & Martin, F. L. (2016). Aluminium foil as a potential substrate for ATR-FTIR, transflection FTIR or Raman spectrochemical analysis of biological specimens. *Analytical Methods*, *8*(3), 481–487.

Cunha, R., Lafeta, L., Fonseca, E. A., Barbosa, A., Romano-Silva, M. A., Vieira, R., Jorio, A., & Malard, L. M. (2021). Nonlinear and vibrational microscopy for label-free characterization of amyloid-β plaques in Alzheimer's disease model. *Analyst*, *146*(9), 2945–2954.

Cutler, E. G. (2019). *Dopamine detection via surface enhanced Raman scattering for Parkinson's disease*. The University of North Carolina at Charlotte.

Cutshaw, G., Uthaman, S., Hassan, N., Kothadiya, S., Wen, X., & Bardhan, R. (2023). The emerging role of Raman spectroscopy as an omics approach for metabolic profiling and biomarker detection toward precision medicine. *Chemical Reviews*, *123*, 8297–8346.

Dekosky, S. T., & Marek, K. (2003). Looking backward to move forward: Early detection of neurodegenerative disorders. *Science*, *302*(5646), 830–834.

Depciuch, J., Tołpa, B., Witek, P., Szmuc, K., Kaznowska, E., Osuchowski, M., Król, P., & Cebulski, J. (2020). Raman and FTIR spectroscopy in determining the chemical changes in healthy brain tissues and glioblastoma tumor tissues. *Spectrochimica Acta. Part A, Molecular and Biomolecular Spectroscopy*, *225*, 117526.

Desroches, J., Jermyn, M., Mok, K., Lemieux-Leduc, C., Mercier, J., St-Arnaud, K., Urmey, K., Guiot, M.-C., Marple, E., Petrecca, K., & Leblond, F. (2015). Characterization of a Raman spectroscopy probe system for intraoperative brain tissue classification. *Biomedical Optics Express*, *6*(7), 2380–2397.

Dhankhar, D., Nagpal, A., Li, R., Chen, J., Cesario, T. C., & Rentzepis, P. M. (2021). Resonance Raman spectra for the in situ identification of bacteria strains and their inactivation mechanism. *Applied Spectroscopy*, *75*(9), 1146–1154.

Dina, N. E., Tahir, M. A., Bajwa, S. Z., Amin, I., Valev, V. K., & Zhang, L. (2023). SERS-based antibiotic susceptibility testing: Towards point-of-care clinical diagnosis. *Biosensors and Bioelectronics*, *219*, 114843.

Dinish, U. S., Balasundaram, G., Chang, Y.-T., & Olivo, M. (2014). Actively targeted in vivo multiplex detection of intrinsic cancer biomarkers using biocompatible SERS nanotags. *Scientific Reports*, *4*, 4075.

Doerfler, W. (1996). Adenoviruses. In S. Baron (Ed.), *Medical Microbiology* (4th ed.). University of Texas Medical Branch at Galveston. https://www.ncbi.nlm.nih.gov/books/NBK8503/

Dugger, B. N., & Dickson, D. W. (2017). Pathology of neurodegenerative diseases. *Cold Spring Harbor Perspectives in Biology*, *9*(7), a028035.

Dunn, A. R., Stout, K. A., Ozawa, M., Lohr, K. M., Hoffman, C. A., Bernstein, A. I., Li, Y., Wang, M., Sgobio, C., Sastry, N., Cai, H., Caudle, W. M., &

Miller, G. W. (2017). Synaptic vesicle glycoprotein 2C (SV2C) modulates dopamine release and is disrupted in Parkinson disease. *Proceedings of the National Academy of Sciences of the United States of America*, *114*(11), E2253–E2262.

Ember, K., Daoust, F., Mahfoud, M., Dallaire, F., Ahmad, E. Z., Tran, T., Plante, A., Diop, M.-K., Nguyen, T., St-Georges-Robillard, A., Ksantini, N., Lanthier, J., Filiatrault, A., Sheehy, G., Beaudoin, G., Quach, C., Trudel, D., & Leblond, F. (2022). Saliva-based detection of COVID-19 infection in a real-world setting using reagent-free Raman spectroscopy and machine learning. *Journal of Biomedical Optics*, *27*(2), 025002.

Fallahzadeh, O., Dehghani-Bidgoli, Z., & Assarian, M. (2018). Raman spectral feature selection using ant colony optimization for breast cancer diagnosis. *Lasers in Medical Science*, *33*(8), 1799–1806.

Fan, Y., Chen, C., Xie, X., Yang, B., Wu, W., Yue, F., Lv, X., & Chen, C. (2022). Rapid noninvasive screening of cerebral ischemia and cerebral infarction based on tear Raman spectroscopy combined with multiple machine learning algorithms. *Lasers in Medical Science*, *37*(1), 417–424.

Faulds, K., Barbagallo, R. P., Keer, J. T., Smith, W. E., & Graham, D. (2004). SERRS as a more sensitive technique for the detection of labelled oligonucleotides compared to fluorescence. *Analyst*, *129*(7), 567–568.

Favoriti, P., Carbone, G., Greco, M., Pirozzi, F., Pirozzi, R. E. M., & Corcione, F. (2016). Worldwide burden of colorectal cancer: A review. *Updates in Surgery*, *68*(1), 7–11.

Feng, S., Wang, W., Tai, I. T., Chen, G., Chen, R., & Zeng, H. (2015). Label-free surface-enhanced Raman spectroscopy for detection of colorectal cancer and precursor lesions using blood plasma. *Biomedical Optics Express*, *6*(9), 3494–3502.

Feng, X., Moy, A. J., Nguyen, H. T. M., Zhang, Y., Zhang, J., Fox, M. C., Sebastian, K. R., Reichenberg, J. S., Markey, M. K., & Tunnell, J. W. (2018). Raman biophysical markers in skin cancer diagnosis. *Journal of Biomedical Optics*, *23*(5), 1–10.

Figueiredo, M. L. B., Martin, C. S., Furini, L. N., Rubira, R. J. G., Batagin-Neto, A., Alessio, P., & Constantino, C. J. L. (2020). Surface-enhanced Raman scattering for dopamine in Ag colloid: Adsorption mechanism and detection in the presence of interfering species. *Applied Surface Science*, *522*, 146466.

Figueroa, B., Nguyen, T., Sotthivirat, S., Xu, W., Rhodes, T., Lamm, M. S., Smith, R. L., John, C. T., Su, Y., & Fu, D. (2019). Detecting and quantifying microscale chemical reactions in pharmaceutical tablets by stimulated Raman scattering microscopy. *Analytical Chemistry*, *91*(10), 6894–6901.

Fu, Y., Huff, T. B., Wang, H.-W., Cheng, J.-X., & Wang, H. (2008). Ex vivo and in vivo imaging of myelin fibers in mouse brain by coherent anti-Stokes Raman scattering microscopy. *Optics Express*, *16*(24), 19396–19409.

Garcia-Beltran, W. F., Lam, E. C., St Denis, K., Nitido, A. D., Garcia, Z. H., Hauser, B. M., Feldman, J., Pavlovic, M. N., Gregory, D. J., Poznansky, M. C., Sigal, A., Schmidt, A. G., Iafrate, A. J., Naranbhai, V., & Balazs, A. B. (2021). Multiple SARS-CoV-2 variants escape neutralization by vaccine-induced humoral immunity. *Cell*, *184*(9), 2372–2383.e9.

Garcia-Leis, A., & Sanchez-Cortes, S. (2021). Label-free detection and self-aggregation of amyloid βpeptides based on plasmonic effects induced by Ag nanoparticles: Implications in Alzheimer's disease diagnosis. *ACS Applied Nano Materials*, *4*, 3565.

Ge, X., Lin, X., Xu, Z., Wei, G., Huang, W., & Lin, D. (2016). Study on nasopharyngeal cancer tissue using surface-enhanced Raman spectroscopy. In Q. Luo, X. Li, Y. Gu, & Y. Tang (Eds.), *Proceedings Vol. 10024*, Optics in health care and biomedical optics VII (p. 1002446). SPIE – International Society for Optics and Photonics.

Githaiga, J. I., Angeyo, H. K., Kaduki, K. A., & Bulimo, W. D. (2020). Chemometrics-enabled Raman spectrometric qualitative determination and assessment of biochemical alterations during early prostate cancer proliferation in model tissue. *Journal of Spectroscopy*, *2020*, 1–15.

Gordon, B. A., Blazey, T. M., Su, Y., Hari-Raj, A., Dincer, A., Flores, S., Christensen, J., Mcdade, E., Wang, G., Xiong, C., Cairns, N. J., Hassenstab, J., Marcus, D. S., Fagan, A. M., Jack, C. R., Hornbeck, R. C., Paumier, K. L., Ances, B. M., Berman, S. B., … Benzinger, T. L. S. (2018). Spatial patterns of neuroimaging biomarker change in individuals from families with autosomal dominant Alzheimer's disease: A longitudinal study. *Lancet Neurology*, *17*(3), 241–250.

Goulart, A. C. C., Silveira, L., Carvalho, H. C., Dorta, C. B., Pacheco, M. T. T., & Zângaro, R. A. (2022). Diagnosing COVID-19 in human serum using Raman spectroscopy. *Lasers in Medical Science*, *37*(4), 2217–2226.

Guevara, E., Torres-Galván, J. C., Ramírez-Elías, M. G., Luevano-Contreras, C., & González, F. J. (2018). Use of Raman spectroscopy to screen diabetes mellitus with machine learning tools. *Biomedical Optics Express*, *9*(10), 4998–5010.

Guo, T., Li, W., Qian, L., Yan, X., Cui, D., Zhao, J., Ni, H., Zhao, X., Zhang, Z., Li, X., Huang, L., & Wang, L. (2020). Highly-selective detection of EGFR mutation gene in lung cancer based on surface enhanced Raman spectroscopy and asymmetric PCR. *Journal of Pharmaceutical and Biomedical Analysis*, *190*, 113522.

Guze, K., Pawluk, H. C., Short, M., Zeng, H., Lorch, J., Norris, C., & Sonis, S. (2015). Pilot study: Raman spectroscopy in differentiating premalignant and malignant oral lesions from normal mucosa and benign lesions in humans. *Head & Neck*, *37*(4), 511–517.

Han, H., Ma, Q., Li, C., Liu, R., Zhao, L., Wang, W., Zhang, P., Liu, X., Gao, G., Liu, F., Jiang, Y., Cheng, X., Zhu, C., & Xia, Y. (2020). Profiling serum cytokines in COVID-19 patients reveals IL-6 and IL-10 are disease severity predictors. *Emerging Microbes & Infections*, *9*(1), 1123–1130.

Han, Q., Lv, L., Wei, J., Lei, X., Lin, H., Li, G., Cao, J., Xie, J., Yang, W., Wu, S., You, J., Lu, J., Liu, P., & Min, J. (2019). Vps4A mediates the localization and exosome release of β-catenin to inhibit epithelial-mesenchymal transition in hepatocellular carcinoma. *Cancer Letters*, *457*, 47–59.

Happillon, T., Untereiner, V., Beljebbar, A., Gobinet, C., Daliphard, S., Cornillet-Lefebvre, P., Quinquenel, A., Delmer, A., Troussard, X., Klossa, J., & Manfait, M. (2015). Diagnosis approach of chronic lymphocytic leukemia on unstained blood smears using Raman microspectroscopy and supervised classification. *Analyst*, *140*(13), 4465–4472.

He, C., Wu, X., Zhou, J., Chen, Y., & Ye, J. (2021). Raman optical identification of renal cell carcinoma via machine learning. *Spectrochimica Acta. Part A, Molecular and Biomolecular Spectroscopy*, *252*, 119520.

Hobro, A. J., Konishi, A., Coban, C., & Smith, N. I. (2013). Raman spectroscopic analysis of malaria disease progression via blood and plasma samples. *Analyst*, *138*(14), 3927–3933.

Hole, A., Jadhav, P., Pansare, K., Noothalapati, H., Deshmukh, A., Gota, V., Chaturvedi, P., & Krishna, C. M. (2022). Salivary Raman spectroscopy: Understanding alterations in saliva of tobacco habitués and oral cancer subjects. *Vibrational Spectroscopy*, *122*, 103414.

Hong, Y., Li, Y., Huang, L., He, W., Wang, S., Wang, C., Zhou, G., Chen, Y., Zhou, X., Huang, Y., Huang, W., Gong, T., & Zhou, Z. (2020). Label-free diagnosis for colorectal cancer through coffee ring-assisted surface-enhanced Raman spectroscopy on blood serum. *Journal of Biophotonics*, *13*(4), e201960176.

Hu, J., Wu, F., Huang, Z., Ma, S., Zhang, J., Yang, J., Han, X., & Xu, G. (2016). Raman spectroscopy analysis of the biochemical characteristics of experimental keratomycosis. *Current Eye Research*, *41*(11), 1408–1413.

Huang, J., Wen, J., Zhou, M., Ni, S., Le, W., Chen, G., Wei, L., Zeng, Y., Qi, D., Pan, M., Xu, J., Wu, Y., Li, Z., Feng, Y., Zhao, Z., He, Z., Li, B., Zhao, S., Zhang, B., … Du, K. (2021). On-site detection of SARS-CoV-2 antigen by deep learning-based surface-enhanced Raman spectroscopy and its biochemical foundations. *Analytical Chemistry*, *93*(26), 9174–9182.

Huang, R., Harmsen, S., Samii, J. M., Karabeber, H., Pitter, K. L., Holland, E. C., & Kircher, M. F. (2016). High precision imaging of microscopic spread of glioblastoma with a targeted ultrasensitive SERRS molecular imaging probe. *Theranostics*, *6*(8), 1075–1084.

Huang, Z., Bergholt, M. S., Zheng, W., Lin, K., Ho, K. Y., Teh, M., & Yeoh, K. G. (2010). In vivo early diagnosis of gastric dysplasia using narrow-band image-guided Raman endoscopy. *Journal of Biomedical Optics*, *15*(3), 037017.

Huang, Z., Teh, S. K., Zheng, W., Lin, K., Ho, K. Y., Teh, M., & Yeoh, K. G. (2010). In vivo detection of epithelial neoplasia in the stomach

using image-guided Raman endoscopy. *Biosensors & Bioelectronics*, *26*(2), 383–389.

Hulvat, M. C. (2020). Cancer incidence and trends. *Surgical Clinics of North America*, *100*(3), 469–481.

Ibrahim, O., Maguire, A., Meade, A. D., Flint, S., Toner, M., Byrne, H. J., & Lyng, F. M. (2017). Improved protocols for pre-processing Raman spectra of formalin fixed paraffin preserved tissue sections. *Analytical Methods*, *9*(32), 4709–4717.

Jadhav, S. A., Biji, P., Panthalingal, M. K., Murali Krishna, C., Rajkumar, S., Joshi, D. S., & Sundaram, N. (2021). Development of integrated microfluidic platform coupled with surface-enhanced Raman spectroscopy for diagnosis of COVID-19. *Medical Hypotheses*, *146*, 110356.

Jayhooni, S. M. H., Short, M., Assadsangabi, B., Hohert, G., Du, C., Zeng, H., & Takahata, K. (2019). Side-viewing endoscopic Raman spectroscopy for angle-resolved analysis of luminal organs. *Advanced Materials Technologies*, *4*(12), 1900364.

Jeong, S., Kim, Y.-I., Kang, H., Kim, G., Cha, M. G., Chang, H., Jung, K. O., Kim, Y.-H., Jun, B.-H., Hwang, D. W., Lee, Y.-S., Youn, H., Lee, Y.-S., Kang, K. W., Lee, D. S., & Jeong, D. H. (2015). Fluorescence-Raman dual modal endoscopic system for multiplexed molecular diagnostics. *Scientific Reports*, *5*, 9455.

Jermyn, M., Mok, K., Mercier, J., Desroches, J., Pichette, J., Saint-Arnaud, K., Bernstein, L., Guiot, M.-C., Petrecca, K., & Leblond, F. (2015). Intraoperative brain cancer detection with Raman spectroscopy in humans. *Science Translational Medicine*, *7*(274), 274ra19.

Ji, M., Arbel, M., Zhang, L., Freudiger, C. W., Hou, S. S., Lin, D., Yang, X., Bacskai, B. J., & Xie, X. S. (2018). Label-free imaging of amyloid plaques in Alzheimer's disease with stimulated Raman scattering microscopy. *Science Advances*, *4*(11), eaat7715.

Jones, R. R., Hooper, D. C., Zhang, L., Wolverson, D., & Valev, V. K. (2019). Raman techniques: Fundamentals and frontiers. *Nanoscale Research Letters*, *14*(1), 231.

Kaewseekhao, B., Nuntawong, N., Eiamchai, P., Roytrakul, S., Reechaipichitkul, W., & Faksri, K. (2020). Diagnosis of active tuberculosis and latent tuberculosis infection based on Raman spectroscopy and surface-enhanced Raman spectroscopy. *Tuberculosis (Edinburgh, Scotland)*, *121*, 101916.

Karabeber, H., Huang, R., Iacono, P., Samii, J. M., Pitter, K., Holland, E. C., & Kircher, M. F. (2014). Guiding brain tumor resection using surface-enhanced Raman scattering nanoparticles and a hand-held Raman scanner. *ACS Nano*, *8*(10), 9755–9766.

Ke, Z.-Y., Ning, Y.-J., Jiang, Z.-F., Zhu, Y.-Y., Guo, J., Fan, X.-Y., & Zhang, Y.-B. (2022). The efficacy of Raman spectroscopy in lung cancer diagnosis: The first diagnostic meta-analysis. *Lasers in Medical Science*, *37*(1), 425–434.

Kelly, J., Patrick, R., Patrick, S., & Bell, S. E. J. (2018). Surface-enhanced Raman spectroscopy for the detection of a metabolic product in the headspace above live bacterial cultures. *Angewandte Chemie (International Edition in English)*, *57*(48), 15686–15690.

Khan, S., Ullah, R., Khan, A., Wahab, N., Bilal, M., & Ahmed, M. (2016). Analysis of dengue infection based on Raman spectroscopy and support vector machine (SVM). *Biomedical Optics Express*, *7*(6), 2249–2256.

Kim, J. A., Wales, D. J., & Yang, G.-Z. (2020). Optical spectroscopy for in vivo medical diagnosis—A review of the state of the art and future perspectives. *Progress in Biomedical Engineering*, *2*(4), 042001.

Kim, Y.-I., Jeong, S., Jung, K. O., Song, M. G., Lee, C.-H., Chung, S.-J., Park, J. Y., Cha, M. G., Lee, S. G., Jun, B.-H., Lee, Y.-S., Hwang, D. W., Youn, H., Kang, K. W., Lee, Y.-S., Jeong, D. H., & Lee, D. S. (2017). Simultaneous detection of EGFR and VEGF in colorectal cancer using fluorescence-Raman endoscopy. *Scientific Reports*, *7*(1), 1035.

Kochan, K., Marzec, K. M., Chruszcz-Lipska, K., Jasztal, A., Maslak, E., Musiolik, H., Chłopicki, S., & Baranska, M. (2013). Pathological changes in the biochemical profile of the liver in atherosclerosis and diabetes assessed by Raman spectroscopy. *Analyst*, *138*(14), 3885–3890.

Kolhatkar, G., Plathier, J., & Ruediger, A. (2018). Nanoscale investigation of materials, chemical reactions, and biological systems by tip enhanced Raman spectroscopy—A review. *Journal of Materials Chemistry C*, *6*, 1307–1319.

Kong, K., Kendall, C., Stone, N., & Notingher, I. (2015). Raman spectroscopy for medical diagnostics – From in-vitro biofluid assays to in-vivo cancer detection. *Advanced Drug Delivery Reviews*, *89*, 121–134.

Krafft, C. (2012). Raman and coherent anti-Stokes Raman scattering microspectroscopy for biomedical applications. *Journal of Biomedical Optics*, *17*(4), 040801.

Krishna, H., Majumder, S. K., Chaturvedi, P., Sidramesh, M., & Gupta, P. K. (2014). In vivo Raman spectroscopy for detection of oral neoplasia: A pilot clinical study. *Journal of Biophotonics*, *7*(9), 690–702.

Krone, N., Hughes, B. A., Lavery, G. G., Stewart, P. M., Arlt, W., & Shackleton, C. H. L. (2010). Gas chromatography/mass spectrometry (GC/MS) remains a pre-eminent discovery tool in clinical steroid investigations even in the era of fast liquid chromatography tandem mass spectrometry (LC/MS/MS). *Journal of Steroid Biochemistry and Molecular Biology*, *121*(3–5), 496–504.

Kucirka, L. M., Lauer, S. A., Laeyendecker, O., Boon, D., & Lessler, J. (2020). Variation in false-negative rate of reverse transcriptase polymerase chain reaction-based SARS-CoV-2 tests by time since exposure. *Annals of Internal Medicine*, *173*(4), 262–267.

Kumar, N., Drozdz, M. M., Jiang, H., Santos, D. M., & Vaux, D. J. (2017). Nanoscale mapping of newly-synthesised phospholipid molecules in a biological cell using tip-enhanced Raman spectroscopy. *Chemical Communications*, *53*(16), 2451–2454.

Kumar, N., Weckhuysen, B. M., Wain, A. J., & Pollard, A. J. (2019). Nanoscale chemical imaging using tip-enhanced Raman spectroscopy. *Nature Protocols*, *14*(4), 1169–1193.

Kumar, P. (2017). Raman spectroscopy as a promising noninvasive tool in brain cancer detection. *Journal of Innovative Optical Health Sciences*, *10*(5), 1730012.

Lee, S., Kim, S., Choo, J., Shin, S. Y., Lee, Y. H., Choi, H. Y., Ha, S., Kang, K., & Oh, C. H. (2007). Biological imaging of HEK293 cells expressing PLCgamma1 using surface-enhanced Raman microscopy. *Analytical Chemistry*, *79*(3), 916–922.

Le Ru, E. C., Meyer, M., & Etchegoin, P. G. (2006). Proof of single-molecule sensitivity in surface enhanced Raman scattering (SERS) by means of a two-analyte technique. *Journal of Physical Chemistry B*, *110*(4), 1944–1948.

Li, J., Li, J., Wang, H., Qi, L.-W., Zhu, Y., & Lai, M. (2019). Tyrosine and glutamine-leucine are metabolic markers of early-stage colorectal cancers. *Gastroenterology*, *157*(1), 257–259.e5.

Li, M., He, H., Huang, G., Lin, B., Tian, H., Xia, K., Yuan, C., Zhan, X., Zhang, Y., & Fu, W. (2021). A novel and rapid serum detection technology for non-invasive screening of gastric cancer based on Raman spectroscopy combined with different machine learning methods. *Frontiers in Oncology*, *11*, 665176.

Li, Q., Hao, C., & Xu, Z. (2017). Diagnosis of breast cancer tissues using 785 nm miniature Raman spectrometer and pattern regression. *Sensors (Basel)*, *17*(3), 627.

Li, Q., He, X., Wang, Y., Liu, H., Xu, D., & Guo, F. (2013). Review of spectral imaging technology in biomedical engineering: Achievements and challenges. *Journal of Biomedical Optics*, *18*(10), 100901.

Li, X. (2012). Spectral analysis of human saliva for detection of lung cancer using surface-enhanced Raman spectroscopy. *Journal of Biomedical Optics*, *17*(3), 037003.

Li, X., Yang, T., Li, C. S., Song, Y., Lou, H., Guan, D., & Jin, L. (2018). Surface enhanced Raman spectroscopy (SERS) for the multiplex detection of Braf, Kras, and Pik3ca mutations in plasma of colorectal cancer patients. *Theranostics*, *8*(6), 1678–1689.

Lin, D., Qiu, S., Huang, W., Pan, J., Xu, Z., Chen, R., Feng, S., Chen, G., Li, Y., Short, M., Zhao, J., Fawzy, Y., & Zeng, H. (2018). Autofluorescence and

white light imaging-guided endoscopic Raman and diffuse reflectance spectroscopy for in vivo nasopharyngeal cancer detection. *Journal of Biophotonics*, *11*(4), e201700251.

Lin, T., Song, Y.-L., Liao, J., Liu, F., & Zeng, T.-T. (2020). Applications of surface-enhanced Raman spectroscopy in detection fields. *Nanomedicine*, *15*, 2971–2989.

Liu, J., Osadchy, M., Ashton, L., Foster, M., Solomon, C. J., & Gibson, S. J. (2017). Deep convolutional neural networks for Raman spectrum recognition: A unified solution. *Analyst*, *142*(21), 4067–4074.

Liu, K., Jin, S., Song, Z., Jiang, L., Ma, L., & Zhang, Z. (2019). Label-free surface-enhanced Raman spectroscopy of serum based on multivariate statistical analysis for the diagnosis and staging of lung adenocarcinoma. *Vibrational Spectroscopy*, *100*, 177–184.

Liu, S., Ma, H., Zhu, J., Han, X. X., & Zhao, B. (2020). Ferrous cytochrome c-nitric oxide oxidation for quantification of protein S-nitrosylation probed by resonance Raman spectroscopy. *Sensors and Actuators B: Chemical*, *308*, 127706.

Lizio, M. G., Boitor, R., & Notingher, I. (2021). Selective-sampling Raman imaging techniques for ex vivo assessment of surgical margins in cancer surgery. *Analyst*, *146*(12), 3799–3809.

Lohumi, S., Kim, M. S., Qin, J., & Cho, B.-K. (2017). Raman imaging from microscopy to macroscopy: Quality and safety control of biological materials. *TrAC Trends in Analytical Chemistry*, *93*, 183–198.

Long, Y., Sanchez-Espiridion, B., Lin, M., White, L., Mishra, L., Raju, G. S., Kopetz, S., Eng, C., Hildebrandt, M. A. T., Chang, D. W., Ye, Y., Liang, D., & Wu, X. (2017). Global and targeted serum metabolic profiling of colorectal cancer progression. *Cancer*, *123*(20), 4066–4074.

Lussier, F., Thibault, V., Charron, B., Wallace, G. Q., & Masson, J.-F. (2020). Deep learning and artificial intelligence methods for Raman and surface-enhanced Raman scattering. *TrAC Trends in Analytical Chemistry*, *124*, 115796.

Lyng, F. M., Traynor, D., Nguyen, T. N. Q., Meade, A. D., Rakib, F., Al-Saady, R., Goormaghtigh, E., Al-Saad, K., & Ali, M. H. (2019). Discrimination of breast cancer from benign tumours using Raman spectroscopy. *PLoS ONE*, *14*(2), e0212376.

Ma, D., Shang, L., Tang, J., Bao, Y., Fu, J., & Yin, J. (2021). Classifying breast cancer tissue by Raman spectroscopy with one-dimensional convolutional neural network. *Spectrochimica Acta. Part A, Molecular and Biomolecular Spectroscopy*, *256*, 119732.

Malini, R., Venkatakrishna, K., Kurien, J., M Pai, K., Rao, L., Kartha, V. B., & Krishna, C. M. (2006). Discrimination of normal, inflammatory, pre-malignant, and malignant oral tissue: A Raman spectroscopy study. *Biopolymers*, *81*(3), 179–193.

Masliah, E., Rockenstein, E., Veinbergs, I., Mallory, M., Hashimoto, M., Takeda, A., Sagara, Y., Sisk, A., & Mucke, L. (2000). Dopaminergic loss and inclusion body formation in alpha-synuclein mice: Implications for neurodegenerative disorders. *Science*, *287*(5456), 1265–1269.

Masson, L. E., O'brien, C. M., Gautam, R., Thomas, G., Slaughter, J. C., Goldberg, M., Bennett, K., Herington, J., Reese, J., Elsamadicy, E., Newton, J. M., & Mahadevan-Jansen, A. (2022). In vivo Raman spectroscopy monitors cervical change during labor. *American Journal of Obstetrics and Gynecology*, *227*(2), 275.e1–275.e14.

Mathé, E. A., Patterson, A. D., Haznadar, M., Manna, S. K., Krausz, K. W., Bowman, E. D., Shields, P. G., Idle, J. R., Smith, P. B., Anami, K., Kazandjian, D. G., Hatzakis, E., Gonzalez, F. J., & Harris, C. C. (2014). Noninvasive urinary metabolomic profiling identifies diagnostic and prognostic markers in lung cancer. *Cancer Research*, *74*(12), 3259–3270.

Matthäus, C., Dochow, S., Egodage, K. D., Romeike, B. F., Brehm, B. R., & Popp, J. (2018). Detection and characterization of early plaque formations by Raman probe spectroscopy and optical coherence tomography: An in vivo study on a rabbit model. *Journal of Biomedical Optics*, *23*(1), 1–6.

Mcgregor, H. C., Short, M. A., Mcwilliams, A., Shaipanich, T., Ionescu, D. N., Zhao, J., Wang, W., Chen, G., Lam, S., & Zeng, H. (2017). Real-time endoscopic Raman spectroscopy for in vivo early lung cancer detection. *Journal of Biophotonics*, *10*(1), 98–110.

Meksiarun, P., Ishigaki, M., Huck-Pezzei, V. A. C., Huck, C. W., Wongravee, K., Sato, H., & Ozaki, Y. (2017). Comparison of multivariate analysis methods for extracting the paraffin component from the paraffin-embedded cancer tissue spectra for Raman imaging. *Scientific Reports*, *7*, 44890.

Meyerhardt, J. A., & Mayer, R. J. (2005). Systemic therapy for colorectal cancer. *New England Journal of Medicine*, *352*(5), 476–487.

Minamoto, T., & Ronai, Z. E. (2001). Gene mutation as a target for early detection in cancer diagnosis. *Critical Reviews in Oncology/Hematology*, *40*(3), 195–213.

Moghimi-Dehkordi, B. (2012). An overview of colorectal cancer survival rates and prognosis in Asia. *World Journal of Gastrointestinal Oncology*, *4*(4), 71–75.

Moor, K., Terada, Y., Taketani, A., Matsuyoshi, H., & Ohtani, K. (2018). Early detection of virus infection in live human cells using Raman spectroscopy. *Journal of Biomedical Optics*, *23*(9), 1–7.

Morris, M. D., & Mandair, G. S. (2011). Raman assessment of bone quality. *Clinical Orthopaedics and Related Research*, *469*(8), 2160–2169.

Mrđenović, D., Ge, W., Kumar, N., & Zenobi, R. (2022). Nanoscale chemical imaging of human cell membranes using tip-enhanced Raman spectroscopy. *Angewandte Chemie*, *134*(43), e202210288.

Mrđenović, D., Tang, Z.-X., Pandey, Y., Su, W., Zhang, Y., Kumar, N., & Zenobi, R. (2023). Regioselective tip-enhanced Raman spectroscopy of lipid membranes with sub-nanometer axial resolution. *Nano Letters*, *23*(9), 3939–3946.

Mulvaney, S. P., & Keating, C. D. (2000). Raman spectroscopy. *Analytical Chemistry*, *72*(12), 145–158.

Nargis, H. F., Nawaz, H., Ditta, A., Mahmood, T., Majeed, M. I., Rashid, N., Muddassar, M., Bhatti, H. N., Saleem, M., Jilani, K., Bonnier, F., & Byrne, H. J. (2019). Raman spectroscopy of blood plasma samples from breast cancer patients at different stages. *Spectrochimica Acta. Part A, Molecular and Biomolecular Spectroscopy*, *222*, 117210.

Neng, J., Li, Y., Driscoll, A. J., Wilson, W. C., & Johnson, P. A. (2018). Detection of multiple pathogens in serum using silica-encapsulated nanotags in a surface-enhanced Raman scattering-based immunoassay. *Journal of Agricultural and Food Chemistry*, *66*(22), 5707–5712.

Nichols, E., Szoeke, C. E. I., Vollset, S. E., Abbasi, N., Abd-Allah, F., Abdela, J., Aichour, M. T. E., Akinyemi, R. O., Alahdab, F., Asgedom, S. W., Awasthi, A., Barker-Collo, S. L., Baune, B. T., Béjot, Y., Belachew, A. B., Bennett, D. A., Biadgo, B., Bijani, A., Bin Sayeed, M. S., … Murray, C. J. L. (2019). Global, regional, and national burden of Alzheimer's disease and other dementias, 1990-2016: A systematic analysis for the Global Burden of Disease Study 2016. *Lancet Neurology*, *18*(1), 88–106.

Nicolson, F., Jamieson, L. E., Mabbott, S., Plakas, K., Shand, N. C., Detty, M. R., Graham, D., & Faulds, K. (2018). Multiplex imaging of live breast cancer tumour models through tissue using handheld surface enhanced spatially offset resonance Raman spectroscopy (SESORRS). *Chemical Communications (Cambridge, England)*, *54*(61), 8530–8533.

Ning, T., Li, H., Chen, Y., Zhang, B., Zhang, F., & Wang, S. (2021). Raman spectroscopy based pathological analysis and discrimination of formalin fixed paraffin embedded breast cancer tissue. *Vibrational Spectroscopy*, *115*, 103260.

O'brien, C. M., Vargis, E., Paria, B. C., Bennett, K. A., Mahadevan-Jansen, A., & Reese, J. (2014). Raman spectroscopy provides a noninvasive approach for determining biochemical composition of the pregnant cervix in vivo. *Acta Paediatrica*, *103*(7), 715–721.

Olanow, C. W., Schapira, A. H. V., & Rascol, O. (2000). Continuous dopamine-receptor stimulation in early Parkinson's disease. *Trends in Neurosciences (TINS)*, *23*(10), S117–S126.

Otange, B. O., Birech, Z., Okonda, J., & Rop, R. (2017). Conductive silver paste smeared glass substrates for label-free Raman spectroscopic detection of HIV-1 and HIV-1 p24 antigen in blood plasma. *Analytical and Bioanalytical Chemistry*, *409*(12), 3253–3259.

Ouyang, L., Ren, W., Zhu, L., & Irudayaraj, J. (2017). Prosperity to challenges: recent approaches in SERS substrate fabrication. *Reviews in Analytical Chemistry*, *36*(1), 20160027.

Paci, E., Ponti, A., Zappa, M., Patriarca, S., Falini, P., Delmastro, G., Bianchi, S., Sapino, A., Vezzosi, V., Senore, C., Crocetti, E., Frigerio, A., Zanetti, R., Del Turco, M. R., & Segnan, N. (2005). Early diagnosis, not differential treatment, explains better survival in service screening. *European Journal of Cancer*, *41*(17), 2728–2734.

Paidi, S. K., Diaz, P. M., Dadgar, S., Jenkins, S. V., Quick, C. M., Griffin, R. J., Dings, R. P. M., Rajaram, N., & Barman, I. (2019). Label-free Raman spectroscopy reveals signatures of radiation resistance in the tumor microenvironment. *Cancer Research*, *79*(8), 2054–2064.

Pandey, Y., Kumar, N., Goubert, G., & Zenobi, R. (2021). Nanoscale chemical imaging of supported lipid monolayers using tip-enhanced Raman spectroscopy. *Angewandte Chemie International Edition*, *60*(35), 19041–19046.

Paraskevaidi, M., Matthew, B. J., Holly, B. J., Hugh, B. J., Thulya, C. P. V., Loren, C., Stjohn, C., Peter, G., Callum, G., Sergei, K. G., Kamila, K., Maria, K., Kássio, L. M. G., Pierre, M.-H. L., Evangelos, P., Savithri, P., John, A. A., Alexandra, S., Marfran, S., … Bayden, W. (2021). Clinical applications of infrared and Raman spectroscopy in the fields of cancer and infectious diseases. *Applied Spectroscopy Reviews*, *56*(8–10), 804–868.

Paraskevaidi, M., Morais, C. L. M., Halliwell, D. E., Mann, D. M. A., Allsop, D., Martin-Hirsch, P. L., & Martin, F. L. (2018). Raman spectroscopy to diagnose Alzheimer's disease and dementia with lewy bodies in blood. *ACS Chemical Neuroscience*, *9*(11), 2786–2794.

Paria, D., Kwok, K. S., Raj, P., Zheng, P., Gracias, D. H., & Barman, I. (2022). Label-free spectroscopic SARS-CoV-2 detection on versatile nanoimprinted substrates. *Nano Letters*, *22*(9), 3620–3627.

Park, J., Hwang, M., Choi, B., Jeong, H., Jung, J.-H., Kim, H. K., Hong, S., Park, J.-H., & Choi, Y. (2017). Exosome classification by pattern analysis of surface-enhanced Raman spectroscopy data for lung cancer diagnosis. *Analytical Chemistry*, *89*(12), 6695–6701.

Pence, I., & Mahadevan-Jansen, A. (2016). Clinical instrumentation and applications of Raman spectroscopy. *Chemical Society Reviews*, *45*(7), 1958–1979.

Pezzotti, G., Boschetto, F., Ohgitani, E., Fujita, Y., Shin-Ya, M., Adachi, T., Yamamoto, T., Kanamura, N., Marin, E., Zhu, W., Nishimura, I., & Mazda, O. (2022). Raman molecular fingerprints of SARS-CoV-2 British variant and the concept of Raman barcode. *Advanced Science (Weinheim, Baden-Württemberg, Germany)*, *9*(3), e2103287.

Pichardo-Molina, J. L., Frausto-Reyes, C., Barbosa-García, O., Huerta-Franco, R., González-Trujillo, J. L., Ramírez-Alvarado, C. A., Gutiérrez-Juárez, G., & Medina-Gutiérrez, C. (2007). Raman spectroscopy and multivariate analysis of serum samples from breast cancer patients. *Lasers in Medical Science*, *22*(4), 229–236.

Prince, M., Wimo, A. G. M., Ali, G. C., Wu, Y. T., & Prina, M. (2015). *World Alzheimer Report 2015: The global impact of dementia*: An *analysis of prevalence, incidence, cost and trends*. Alzheimer's Disease International.

Qi, Y., Yang, L., Liu, B., Liu, L., Liu, Y., Zheng, Q., Liu, D., & Luo, J. (2021). Accurate diagnosis of lung tissues for 2D Raman spectrogram by deep learning based on short-time Fourier transform. *Analytica Chimica Acta*, *1179*, 338821.

Qian, K., Wang, Y., Hua, L., Chen, A., & Zhang, Y. (2018). New method of lung cancer detection by saliva test using surface-enhanced Raman spectroscopy. *Thoracic Cancer*, *9*(11), 1556–1561.

Rabbani, G., & Ahn, S. N. (2021). Review: Roles of human serum albumin in prediction, diagnoses and treatment of COVID-19. *International Journal of Biological Macromolecules*, *193*(Pt A), 948–955.

Ralbovsky, N. M., Halámková, L., Wall, K., Anderson-Hanley, C., & Lednev, I. K. (2019). Screening for Alzheimer's disease using saliva: A new approach based on machine learning and Raman hyperspectroscopy. *Journal of Alzheimer's Disease*, *71*(4), 1351–1359.

Rangaraju, L. P., Kunapuli, G., Every, D., Ayala, O. D., Ganapathy, P., & Mahadevan-Jansen, A. (2019). Classification of burn injury using Raman spectroscopy and optical coherence tomography: An ex-vivo study on porcine skin. *Burns*, *45*(3), 659–670.

Ren, X., Zhang, Q., Yang, J., Zhang, X., Zhang, X., Zhang, Y., Huang, L., Xu, C., Ge, Y., Chen, H., Liu, X., & Wang, Y. (2021). Dopamine imaging in living cells and retina by surface-enhanced Raman scattering based on functionalized gold nanoparticles. *Analytical Chemistry*, *93*(31), 10841–10849.

Riva, M., Sciortino, T., Secoli, R., D'amico, E., Moccia, S., Fernandes, B., Conti Nibali, M., Gay, L., Rossi, M., De Momi, E., & Bello, L. (2021). Glioma biopsies classification using Raman spectroscopy and machine learning models on fresh tissue samples. *Cancers (Basel)*, *13*(5), 1073.

Robert, B. (2009). Resonance Raman spectroscopy. *Photosynthesis Research*, *101*(2–3), 147–155.

Rojalin, T., Phong, B., Koster, H. J., & Carney, R. P. (2019). Nanoplasmonic approaches for sensitive detection and molecular characterization of extracellular vesicles. *Frontiers in Chemistry*, *7*, 279.

Rostron, P., & Gerber, D. (2016). Raman spectroscopy, a review. *International Journal of Engineering and Technical Research*, *6*, 50–64.

Ruan, S. (2020). Likelihood of survival of coronavirus disease 2019. *The Lancet Infectious Diseases*, *20*(6), 630–631.

Rubina, S., & Krishna, C. M. (2015). Raman spectroscopy in cervical cancers: An update. *Journal of Cancer Research and Therapeutics*, *11*(1), 10–17.

Ryzhikova, E., Kazakov, O., Halamkova, L., Celmins, D., Malone, P., Molho, E., Zimmerman, E. A., & Lednev, I. K. (2015). Raman spectroscopy of blood serum for Alzheimer's disease diagnostics: Specificity relative to other types of dementia. *Journal of Biophotonics*, *8*(7), 584–596.

Ryzhikova, E., Ralbovsky, N. M., Sikirzhytski, V., Kazakov, O., Halamkova, L., Quinn, J., Zimmerman, E. A., & Lednev, I. K. (2021). Raman spectroscopy and machine learning for biomedical applications: Alzheimer's disease diagnosis based on the analysis of cerebrospinal fluid. *Spectrochimica Acta. Part A, Molecular and Biomolecular Spectroscopy*, *248*, 119188.

Santos, I. P., Barroso, E. M., Bakker Schut, T. C., Caspers, P. J., Van Lanschot, C. G. F., Choi, D.-H., Van Der Kamp, M. F., Smits, R. W. H., Van Doorn, R., Verdijk, R. M., Noordhoek Hegt, V., Von Der Thüsen, J. H., Van Deurzen, C. H. M., Koppert, L. B., Van Leenders, G. J. L. H., Ewing-Graham, P. C., Van Doorn, H. C., Dirven, C. M. F., Busstra, M. B., … Koljenović, S. (2017). Raman spectroscopy for cancer detection and cancer surgery guidance: Translation to the clinics. *Analyst*, *142*(17), 3025–3047.

Sciortino, T., Secoli, R., D'amico, E., Moccia, S., Conti Nibali, M., Gay, L., Rossi, M., Pecco, N., Castellano, A., De Momi, E., Fernandes, B., Riva, M., & Bello, L. (2021). Raman spectroscopy and machine learning for IDH genotyping of unprocessed glioma biopsies. *Cancers (Basel)*, *13*(16), 4196.

Sebba, D., Lastovich, A. G., Kuroda, M., Fallows, E., Johnson, J., Ahouidi, A., Honko, A. N., Fu, H., Nielson, R., Carruthers, E., Diédhiou, C., Ahmadou, D., Soropogui, B., Ruedas, J., Peters, K., Bartkowiak, M., Magassouba, N., Mboup, S., Ben Amor, Y., … Weidemaier, K. (2018). A point-of-care diagnostic for differentiating Ebola from endemic febrile diseases. *Science Translational Medicine*, *10*(471), eaat0944.

Shin, H., Jeong, H., Park, J., Hong, S., & Choi, Y. (2018). Correlation between cancerous exosomes and protein markers based on surface-enhanced Raman spectroscopy (SERS) and principal component analysis (PCA). *ACS Sensors*, *3*(12), 2637–2643.

Shin, H., Oh, S., Hong, S., Kang, M., Kang, D., Ji, Y.-G., Choi, B. H., Kang, K.-W., Jeong, H., Park, Y., Hong, S., Kim, H. K., & Choi, Y. (2020). Early-stage lung cancer diagnosis by deep learning-based spectroscopic analysis of circulating exosomes. *ACS Nano*, *14*(5), 5435–5444.

Shiratori, I., Akitomi, J., Boltz, D. A., Horii, K., Furuichi, M., & Waga, I. (2014). Selection of DNA aptamers that bind to influenza A viruses with high affinity and broad subtype specificity. *Biochemical and Biophysical Research Communications*, *443*(1), 37–41.

Short, M. A., Wang, W., Tai, I. T., & Zeng, H. (2016). Development and in vivo testing of a high frequency endoscopic Raman spectroscopy system for potential applications in the detection of early colonic neoplasia. *Journal of Biophotonics*, *9*(1–2), 44–48.

Shrestha, G. S., Kwizera, A., Lundeg, G., Baelani, J. I., Azevedo, L. C. P., Pattnaik, R., Haniffa, R., Gavrilovic, S., Mai, N. T. H., Kissoon, N., Lodha,

R., Misango, D., Neto, A. S., Schultz, M. J., Dondorp, A. M., Thevanayagam, J., Dünser, M. W., Alam, A. K. M. S., Mukhtar, A. M., … Mer, M. (2017). International Surviving Sepsis Campaign guidelines 2016: The perspective from low-income and middle-income countries. *The Lancet Infectious Diseases*, *17*(9), 893–895.

Shu, C., Zheng, W., Lin, K., Lim, C., & Huang, Z. (2021). Label-free follow-up surveying of post-treatment efficacy and recurrence in nasopharyngeal carcinoma patients with fiberoptic Raman endoscopy. *Analytical Chemistry*, *93*(4), 2053–2061.

Singh, S. P., Sahu, A., Deshmukh, A., Chaturvedi, P., & Krishna, C. M. (2013). In vivo Raman spectroscopy of oral buccal mucosa: A study on malignancy associated changes (MAC)/cancer field effects (CFE). *Analyst*, *138*(14), 4175–4182.

Sitjar, J., Liao, J.-D., Lee, H., Tsai, H.-P., Wang, J.-R., & Liu, P.-Y. (2021). Challenges of SERS technology as a non-nucleic acid or -antigen detection method for SARS-CoV-2 virus and its variants. *Biosensors & Bioelectronics*, *181*, 113153.

Sivashanmugan, K., Huang, W.-L., Lin, C.-H., Liao, J.-D., Lin, C.-C., Su, W.-C., & Wen, T.-C. (2017). Bimetallic nanoplasmonic gap-mode SERS substrate for lung normal and cancer-derived exosomes detection. *Journal of the Taiwan Institute of Chemical Engineers*, *80*, 149–155.

Smith, R., Wright, K. L., & Ashton, L. (2016). Raman spectroscopy: An evolving technique for live cell studies. *Analyst*, *141*(12), 3590–3600.

Song, D., Chen, T., Wang, S., Chen, S., Li, H., Yu, F., Zhang, J., & Zhang, Z. (2020). Study on the biochemical mechanisms of the micro-wave ablation treatment of lung cancer by ex vivo confocal Raman microspectral imaging. *Analyst*, *145*(2), 626–635.

Sonntag, M. D., Pozzi, E. A., Jiang, N., Hersam, M. C., & Van Duyne, R. P. (2014). Recent advances in tip-enhanced Raman spectroscopy. *Journal of Physical Chemistry Letters*, *5*(18), 3125–3130.

Su, X., Xie, Y., Liu, X., Chen, M., Zheng, C., Zhong, H., & Li, M. (2023). Absolute quantification of serum exosomes in patients with an SERS-lateral flow strip biosensor for noninvasive clinical cancer diagnosis. *ACS Applied Materials & Interfaces*, *15*(31), 37130–37142.

Sung, H., Ferlay, J., Siegel, R. L., Laversanne, M., Soerjomataram, I., Jemal, A., & Bray, F. (2021). Global cancer statistics 2020: GLOBOCAN estimates of incidence and mortality worldwide for 36 cancers in 185 countries. *CA: A Cancer Journal for Clinicians*, *71*(3), 209–249.

Tabatabaei, M., Caetano, F. A., Pashee, F., Ferguson, S. S. G., & Lagugné-Labarthet, F. (2017). Tip-enhanced Raman spectroscopy of amyloid β at neuronal spines. *Analyst*, *142*(23), 4415–4421.

Tahir, M. A., Dina, N. E., Cheng, H., Valev, V. K., & Zhang, L. (2021). Surface-enhanced Raman spectroscopy for bioanalysis and diagnosis. *Nanoscale*, *13*(27), 11593–11634.

Talaga, D., Smeralda, W., Lescos, L., Hunel, J., Lepejova-Caudy, N., Cullin, C., Bonhommeau, S., & Lecomte, S. (2018). PIP(2) phospholipid-induced aggregation of tau filaments probed by tip-enhanced Raman spectroscopy. *Angewandte Chemie (International Edition in English)*, *57*(48), 15738–15742.

Thomas, G. J. (1976). Raman spectroscopy and virus research. *Applied Spectroscopy*, *30*(5), 483–494.

Tien, N., Lin, T.-H., Hung, Z.-C., Lin, H.-S., Wang, I.-K., Chen, H.-C., & Chang, C.-T. (2018). Diagnosis of bacterial pathogens in the urine of urinary-tract-infection patients using surface-enhanced Raman spectroscopy. *Molecules (Basel, Switzerland)*, *23*(12), 3374.

Traynor, D., Martin, C. M., White, C., Reynolds, S., D'arcy, T., O'leary, J. J., & Lyng, F. M. (2021). Raman spectroscopy of liquid-based cervical smear samples as a triage to stratify women who are HPV-positive on screening. *Cancers (Basel)*, *13*(9), 2008.

Van Heel, A. C. S. (1954). A new method of transporting optical images without aberrations. *Nature*, *173*(4392), 39–39.

Váradi, L., Luo, J. L., Hibbs, D. E., Perry, J. D., Anderson, R. J., Orenga, S., & Groundwater, P. W. (2017). Methods for the detection and identification of pathogenic bacteria: Past, present, and future. *Chemical Society Reviews*, *46*(16), 4818–4832.

Vardaki, M. Z., Pavlou, E., Simantiris, N., Lampri, E., Seretis, K., & Kourkoumelis, N. (2023). Towards non-invasive monitoring of non-melanoma skin cancer using spatially offset Raman spectroscopy. *Analyst*, *148*(18), 4386–4395.

Verma, P. (2017). Tip-enhanced Raman spectroscopy: Technique and recent advances. *Chemical Reviews*, *117*(9), 6447–6466.

Verroken, A., Defourny, L., Lechgar, L., Magnette, A., Delmée, M., & Glupczynski, Y. (2015). Reducing time to identification of positive blood cultures with MALDI-TOF MS analysis after a 5-h subculture. *European Journal of Clinical Microbiology & Infectious Diseases*, *34*(2), 405–413.

Vila, M., Vukosavic, S., Jackson-Lewis, V., Neystat, M., Jakowec, M., & Przedborski, S. (2000). Alpha-synuclein up-regulation in substantia nigra dopaminergic neurons following administration of the parkinsonian toxin MPTP. *Journal of Neurochemistry*, *74*(2), 721–729.

Wang, H., Zhang, S., Wan, L., Sun, H., Tan, J., & Su, Q. (2018). Screening and staging for non-small cell lung cancer by serum laser Raman spectroscopy. *Spectrochimica Acta. Part A, Molecular and Biomolecular Spectroscopy*, *201*, 34–38.

Wang, J., Lin, K., Zheng, W., Ho, K. Y., Teh, M., Yeoh, K. G., & Huang, Z. (2015). Comparative study of the endoscope-based bevelled and volume fiber-optic Raman probes for optical diagnosis of gastric dysplasia in vivo at endoscopy. *Analytical and Bioanalytical Chemistry*, *407*(27), 8303–8310.

Wang, J., Lin, K., Zheng, W., Ho, K. Y., Teh, M., Yeoh, K. G., & Huang, Z. (2015). Simultaneous fingerprint and high-wavenumber fiber-optic Raman spectroscopy improves in vivo diagnosis of esophageal squamous cell carcinoma at endoscopy. *Scientific Reports*, *5*(1), 12957.

Wang, X., Huang, S.-C., Huang, T.-X., Su, H.-S., Zhong, J.-H., Zeng, Z.-C., Li, M.-H., & Ren, B. (2017). Tip-enhanced Raman spectroscopy for surfaces and interfaces. *Chemical Society Reviews*, *46*(13), 4020–4041.

Wang, Z., Ye, J., Zhang, K., Ding, L., Granzier-Nakajima, T., Ranasinghe, J. C., Xue, Y., Sharma, S., Biase, I., Terrones, M., Choi, S. H., Ran, C., Tanzi, R. E., Huang, S. X., Zhang, C., & Huang, S. (2022). Rapid biomarker screening of Alzheimer's disease by interpretable machine learning and graphene-assisted Raman spectroscopy. *ACS Nano*, *16*(4), 6426–6436.

Wu, W., Yu, X., Wu, J., Wu, T., Fan, Y., Chen, W., Zhao, M., Wu, H., Li, X., & Ding, S. (2021). Surface plasmon resonance imaging-based biosensor for multiplex and ultrasensitive detection of NSCLC-associated exosomal miRNAs using DNA programmed heterostructure of Au-on-Ag. *Biosensors & Bioelectronics*, *175*, 112835.

Xiao, M., Xie, K., Dong, X., Wang, L., Huang, C., Xu, F., Xiao, W., Jin, M., Huang, B., & Tang, Y. (2019). Ultrasensitive detection of avian influenza A (H7N9) virus using surface-enhanced Raman scattering-based lateral flow immunoassay strips. *Analytica Chimica Acta*, *1053*, 139–147.

Xu, R., Cui, B., Duan, X., Zhang, P., Zhou, X., & Yuan, Q. (2020). Saliva: Potential diagnostic value and transmission of 2019-nCoV. *International Journal of Oral Science*, *12*(1), 11.

Yala, A., Lehman, C., Schuster, T., Portnoi, T., & Barzilay, R. (2019). A deep learning mammography-based model for improved breast cancer risk prediction. *Radiology*, *292*(1), 60–66.

Yamamoto, S., Kaimori, J.-Y., Yoshimura, T., Namba, T., Imai, A., Kobayashi, K., Imamura, R., Ichimaru, N., Kato, K., Nakaya, A., Takahara, S., & Isaka, Y. (2017). Analysis of an ADTKD family with a novel frameshift mutation in MUC1 reveals characteristic features of mutant MUC1 protein. *Nephrology, Dialysis, Transplantation*, *32*(12), 2010–2017.

Yang, T., Guo, X., Wu, Y., Wang, H., Fu, S., Wen, Y., & Yang, H. (2014). Facile and label-free detection of lung cancer biomarker in urine by magnetically assisted surface-enhanced Raman scattering. *ACS Applied Materials & Interfaces*, *6*(23), 20985–20993.

Yin, G., Li, L., Lu, S., Yin, Y., Su, Y., Zeng, Y., Luo, M., Ma, M., Zhou, H., Orlandini, L., Yao, D., Liu, G., & Lang, J. (2021). An efficient primary screening of COVID-19 by serum Raman spectroscopy. *Journal of Raman Spectroscopy*, *52*(5), 949–958.

Yuen, C. (2012). Magnetic field enriched surface enhanced resonance Raman spectroscopy for early malaria diagnosis. *Journal of Biomedical Optics*, *17*(1), 017005.

Zhang, B., Xu, H., Chen, J., Zhu, X., Xue, Y., Yang, Y., Ao, J., Hua, Y., & Ji, M. (2021). Highly specific and label-free histological identification of microcrystals in fresh human gout tissues with stimulated Raman scattering. *Theranostics*, *11*(7), 3074–3088.

Zhang, C., Leng, W., Sun, C., Lu, T., Chen, Z., Men, X., Wang, Y., Wang, G., Zhen, B., & Qin, J. (2018). Urine proteome profiling predicts lung cancer from control cases and other tumors. *EBioMedicine*, *30*, 120–128.

Zhang, J. J., Wang, N., Wang, H., Zhou, W., Xu, X., Zeng, Q., & Chen, X. (2022). Feasibility demonstration of supercontinuum fiber laser-based coherent anti-Stokes Raman scattering microscopy. *Proceedings Vol. 11973*, Advanced *chemical microscopy for life science and translational medi*cine 2022 (p. 1197307). SPIE – International Society for Optics and Photonics.

Zhang, K., Hao, C., Man, B., Zhang, C., Yang, C., Liu, M., Peng, Q., & Chen, C. (2018). Diagnosis of liver cancer based on tissue slice surface enhanced Raman spectroscopy and multivariate analysis. *Vibrational Spectroscopy*, *98*, 82–87.

Zhang, L., Su, Y., Liang, X., Cao, K., Luo, Q., & Luo, H. (2023). Ultrasensitive and point-of-care detection of plasma phosphorylated tau in Alzheimer's disease using colorimetric and surface-enhanced Raman scattering dual-readout lateral flow assay. *Nano Research*, *16*, 7459–7469.

Zhang, L., Li, C., Peng, D., Yi, X., He, S., Liu, F., Zheng, X., Huang, W. E., Zhao, L., & Huang, X. (2022). Raman spectroscopy and machine learning for the classification of breast cancers. *Spectrochimica Acta. Part A, Molecular and Biomolecular Spectroscopy*, *264*, 120300.

Zikic, B., Bremner, A., Talaga, D., Lecomte, S., & Bonhommeau, S. (2021). Tip-enhanced Raman spectroscopy of Aβ(1-42) fibrils. *Chemical Physics Letters*, *768*, 138400.

How to cite this article: Qi, Y., Chen, E. X., Hu, D., Yang, Y., Wu, Z., Zheng, M., Sadi, M. A., Jiang, Y., Zhang, K., Chen, Z., & Chen, Y. P. (2024). Applications of Raman spectroscopy in clinical medicine. *Food Frontiers*, 1–28.
https://doi.org/10.1002/fft2.335